▼ 📁 Abstracts Posters K-R first authors

- 📄 Lea 1991 PEO modified Cantilevers AFM Int. Conf 10 Years STM Hlady .pdf
- 📄 Lee Hai Bang 1974 Dissertation Abstract Water in Hydrogel PHEMA
- 📄 Lee HB 1988 Adhesion Gradient Surfaces 3rd World Biomaterials Con Kyoto Japan-.pdf
- 📄 Lin 1985 Evanescent Immunosensors Electrochem Soc. Las Vegas Hlady Reichert.pdf
- 📄 Lin 1987 JN Ag-Ab on silica 40th ACEMB.pdf
- 📄 Lin 1988 JN FluoroImmunoAssay EPA Army Field Screening.pdf
- 📄 Lin 1988 Photoregulation Ag-Ab Sensors Kyoto Kopeckova 3rd World Biomaterials Herron
- 📄 Lin 1990 Soc Biomaterials Immunoglobulin on Mica AFM Drake Lea Hansma.pdf
- 📄 Marchant 1991 Soc. Biomaterials Von Willebrand on Mica AFM Lea.pdf
- 📄 Mohan poster 9-05
- 📄 Quinn 1982 MSc Thesis abstract Insulin .pdf
- 📄 Ramirez 1974 Dissertation Abst chelating polymers .pdf
- 📄 Reichert 1985 soc biomaterials evanescent streak newby.pdf
- 📄 Reinecke 1984 Adsorption Gamma TIRF World Biomaterials van wagenen smith WashDC .pdf
- 📄 Rickel 1986 Biomaterials soc Adorption lipoproteins hlady .pdf
- 📄 Russell 1977 Relaxations Methacrylates Hiltner Amer Phys Soc

Ab Lea - 2

STM 91

2F/42

AFM IMAGING USING POLYETHYLENEOXIDE MODIFIED CANTILEVERS

A. S. Lea, V. Hlady and J. D. Andrade: Department of Bioengineering, University of Utah, Salt Lake City, UT 84112, USA.

In aqueous systems, surfaces covered with polyethyleneoxide (PEO) repel each other when brought together due to the steric exclusion forces manifested by the extended polymer chains (1). AFM cantilever tips coated with PEO would enable imaging in aqueous environments to be accomplished using predominately steric exclusion forces. The potential for the use of these cantilevers to minimize the lateral translation of surface adsorbed entities (2) will be presented with emphasis on PEO surface coverage and molecular weight.

Silicon nitride cantilevers were modified by chemically coupling PEO of specified molecular weights to their surface. The coupling procedure was monitored by ESCA and electrophoretic mobility and PEO layer thicknesses were determined by ellipsometry. The force curves were similar to those obtained using the surface force apparatus (1): steric exclusion forces commencing at a separation distance of ~6 R_g (the solution mean radius of gyration of the random polymer coil) and dominating the attractive van der Waals forces at smaller separations. At large separations there is considerable loss of resolution due to the slow development of the exponential steric exclusion force (3). At smaller separations, the resolution is greater. We are currently investigating the potential of these tips to minimize perturbation of surface adsorbed gold particles and proteins.

1. Klein J. and Luckham P., *Nature* 300 429 (1982).
2. Lea A.S., Pungor A., Hlady V., Andrade J.D., Herron J.N. and Voss, Jr. E.W., submitted to *Langmuir*, February 1991.
3. Jeon S.I., Lee J.H., Andrade J.D. and de Gennes P.G., *J. Coll. Interf. Sci.* 142 149, 159 (1990).

2F/43

A DETAILED ANALYSIS OF THE OPTICAL BEAM DEFLECTION TECHNIQUE.

C.A.J. Putman, B.G. De Grooth, N.F. Van Hulst, K.O. Van der Werf, J. Greve: Department of Applied Physics, Twente University, P.O. BOX 217 7500 AE Enschede, The Netherlands.

In Atomic Force Microscopy (AFM) minute displacements of a small cantilever are measured. The most widely used methods for the detection of the change in cantilever position are (fiber)interferometry and optical beam deflection. At first sight, most physicist would expect the interferometric based techniques to be much more sensitive than the beam deflection method. In practice, however, images with atomic resolution have been obtained while using the optical beam deflection method.

We will present a detailed theoretical analysis of the beam deflection method. Several optical configurations, e.g. laser beam focused at cantilever or at position sensitive detector, will be discussed within practical boundary conditions. The analysis explains that, while using a 1 mW laser diode, the signal-to-noise ratio in a 10 kHz bandwidth is sufficiently high to achieve atomic resolution. The theoretical predictions are compared with experimental results.

In all practical situations, the signal-to-noise ratio of the optical beam deflection method is comparable to that of the more complex interferometric techniques.

International Conf. on STM, Interlaken, Aug 12-16, 1991 Under the auspices of the European Physical Society

---

3F/29

AN AFM STUDY OF POLYSTYRENE LATEX PARTICLES AS A CALIBRATION STANDARD.

Y. Li, J. Pan and S.M. Lindsay

Department of Physics, Arizona State University, Tempe, AZ 85287, USA

Atomic Force Microscopy (AFM) has the ability to image conducting and, more importantly, non-conducting surfaces with atomic resolution. We have used AFM to investigate sub-monolayer to multiple layer coverage of polystyrene latex particles on various surfaces. Latex spheres with diameters ranging from 60 nm to 500 nm were studied. The distribution of the sphere sizes was consistent with independent measurements. The latex spheres were observed to pack into both ordered and disordered structures. The packing structure depends on such factors as particle concentration and size distribution. We have dispersed latex particles onto various substrates and have observed that "particle-substrate" interactions play an important role in film formation. The polystyrene latex spheres provide a simple way to calibrate AFM instruments in x, y and z directions simultaneously. AFM images of various latex spheres will be presented.

Ab Stroup - 3

STM 91

3F/30

ELASTICITY MAPPING OF POLYMER SURFACES WITH AFM

E.W. Stroup, A.S. Lea, A. Pungor, V. Hlady, J.D. Andrade: Department of Bioengineering, University of Utah Salt Lake City, Utah 84112 USA

The elastic nature of samples being imaged with AFM is of great interest. If the sample is very elastic, it may deform under the force of the tip. This deformation may cause increased surface contact area between the tip and the sample thereby producing a convoluted topographical image. However, the elastic nature of the surface can be used as an advantage to map the "hardness" of the surface.

The AFM has been used to image polymer surfaces to produce a "hardness map" from differences in surface elasticities, in contrast to a topographical image of variances in height. To accomplish this imaging, the AFM is used in the force modulation mode. When activated, the piezoelectric crystal controlling the sample holder moves in the z direction and causes the cantilever to deflect from its original position, z_d. The deflection, Δz_d, is used in a ratio with the change in height of the piezo, Δz_m, to create an image. This mode allows the AFM to recognize soft sections in relation to hard sections, since the change in the deflection of the cantilever will be related to the hardness of the area under the tip (1). We have used this technique to image the surfaces of graphite fibers in a polycarbonate matrix, and copolymers of styrenebutadiene. The contrast in the elasticities of the components of the samples is revealed through the force modulation method.

1. P.Maivald, H.-J. Butt, A.S. Gould, C.B. Prater, B. Drake, J.A. Gurley, V.B. Elings, and P.K. Hansma, Submitted to Nanotechnology,1991.

STM'91 Abstracts, International Conf. on STM, Interlaken, August 12-16, 1991 - under auspices of the European Physical Society

S-M '91

Abstracts

10 Years of STM

International Conference on
Scanning Tunneling Microscopy
Interlaken, August 12-16, 1991

Under the auspices of the European Physical Society

larger differences in the female population than in the male population.

For the second approach, the first four central moments at each time point of the responses were evaluated for the entire data base. The results indicated stimulus-related changes in the first central moment and, in some cases, in the second central moment. Stimuli-related changes in the second moment confirmed the reported alpha blocking phenomena. The third and fourth moments representing skewness and kurtosis showed no significant stimulus-related behavior.

To get an indication of the extent to which the evoked response carries information about the stimulus that evoked it, the correlation function evaluated at zero time lag, $\tau = 0$, was calculated between all evoked responses and the signal (sample mean). The resulting correlation coefficients obtained were z transformed and averaged. Since there were 7 stimulus types and 7 signals, the averaged z values formed a 7 x 7 matrix for each subject. The matrices, on the average, showed maximal correlation between a given response type and its own signal indicating recognition of the response by its estimated signal. In general, the correlation coefficients obtained for the female population was higher than for the male population.

The correlation coefficients obtained for a given response when correlated with all 7 signal types were also compared. When the coefficient between the response and its own signal was largest, it was called a hit; otherwise, it was a miss. The percent of hits for all response types was calculated showing level of significances of the order $p \leq 10^{-6}$.

Order No. 74-21,547, 202 pages.

THE NATURE OF WATER IN A SYNTHETIC HYDROGEL: POLY(2-HYDROXYETHYL METHACRYLATE)

LEE, Hai-Bang, Ph.D.
University of Utah, 1974

Chairman: Joseph D. Andrade

The possible role of water in the interfacial and biological properties of gels is briefly discussed in order to test the hypothesis that water is not merely a passive medium or milieu in which biochemical reactions and physiological processes occur. A hypothesis that three classes of water exist in hydrogels, namely X water (bulk water), Z water (bound water), and Y water (intermediate forms we call interfacial water), is proposed, and verified by a number of experiments.

Bulk gel conductivity data for poly(2-hydroxyethyl methacrylate) (PHEMA) gel was obtained. The activation energy for specific conduction was obtained from the relation

$$\log K = \text{const} - \frac{\Delta E_a}{2.303\,RT}$$

where K is the specific conductivity and ΔE_a is the activation energy for conduction. A plot of the activation energy vs. wt % of water in the gels clearly indicated three different zones, showing three possible classes of water in the gels. These results were confirmed by thermal expansion measurements. The high water content gels (50%) showed an extremely sharp volume change at 0°C, indicating the presence of normal bulk water. Lower content gels (20%) showed no anomalous change in thermal expansion, indicating that the water is bound. The medium water content gels exhibited intermediate behavior. A semi-quantitative analysis of the three classes of water is presented.

The third method used in this research was the differential scanning calorimetry (DSC) technique. The lower water con-

tent gel (20%) consisted mainly of bound water, which exhibits no phase transitions over the temperature range of -20 to 24°C. The higher water content gels showed phase transitions near 0°C. The medium water content gels showed gradual shifts of the phase transition temperatures near 0°C. The effect of crosslinker concentration was studied by DSC.

To further verify the hypothesis, the spin-lattice nuclear magnetic relaxation time (T_1) of protons in the PHEMA gels as a function of non-equilibrium water content from 20 to 60% was measured at 20 MHz at 34°C.

A simplified model of PHEMA gels is employed in which local proton relaxation times were assigned to three different classes of water: 1) bound water near the polymer network, 2) interfacial water near the bound water, and 3) bulk water or water unaffected by the network. The activation energies for interchange among the three classes of water were calculated from the relaxation time data. Our calculated values for interchange between bound water and bulk water, and between interfacial water and bulk water, are 2.5 and 2.0 Kcal/mole, respectively. These values are reasonable in that the activation energy for viscous flow of water is approximately 4 Kcal/mole at 34°C. The correlation time for PHEMA-bound water, 2.3×10^{-10}s, and PHEMA-interfacial water, 8×10^{-11}s, are about 75 and 27 times, respectively, longer than that for pure water (3×10^{-12}s). The water with longer correlation times may have a more ordered structure in the polymer network than bulk water.

Additional work reported here includes radiation grafting and protein adsorption on PHEMA gels.

Order No. 74-22,240, 120 pages.

THE MICROCIRCULATION: THEORY AND EXPERIMENT

MAYROVITZ, Harvey Norman, Ph.D.
University of Pennsylvania, 1974

Supervisors: Abraham Noordergraff and
Lysle H. Peterson

Using the bat wing as an experimental preparation and as a prototype of a self contained vascular bed, a Microvascular Model was developed. Together with theoretical analysis and pertinent experimental data it was used to help interpret and quantify a number of aspects of microcirculatory function.

METHODS

The number, dimensions, and distribution of the vessels of the real vascular bed were included into an analyzable, representative geometric configuration. Equations were developed and utilized to characterize the pressure-flow relationships for each branching order of the vascular field. The configuration and describing equations (termed Topological Model) were used to evaluate the vascular bed resistance distribution. In addition the Topological Model formed the framework on which an extensive computer based Microvascular Model was built. It included the macroscopic properties of the vascular bed and, in addition, a detailed representation of precapillary vessel dynamics (vasomotion), capillary hemodynamics and filtration, and postcapillary dynamics (venomotion). In vivo comparisons including pressure distribution and propagation characteristics served to test the accuracy of the Microvascular Model prior to its use to interpret the functional significance of vasomotion and venomotion to the capillary level.

CELL ADHESION ON GRADIENT SURFACES

H.B. LEE AND J.D. ANDRADE.

KOREA RESEARCH INSTITUTE OF CHEMICAL TECHNOLOGY
P.O. BOX 9, DAE-DEOG, CHUNGNAM, KOREA

INTRODUCTION - The investigation of cell adhesion on polymeric materials has been emphasized in the applications of biomedical science and devices including biology, medicine and biotechnology. Bacterial cells adhesion to surfaces is also a common phenomenon. van Wachem, et al (1) reported the interaction of cells to thirteen different polymer surfaces. They concluded that optimal adhesion of human endothelial cells occurred to polymer surfaces as a function of wettability. Tanzawa, et al (2) also investigated that cell adhesion and growth on the surfaces of synthetic hydrogels which have different water contents. The result shows that the number of cell adhering to the hydrogels decreased with increasing water content. These studies are performed one surface at a time. The systematic study of the effect of one surface parameter on cell adhesion requires many different samples, each with a different value of the surface parameter of interest. In order to reduce experimental parameters, it is desirable to produce gradient of surface properties on one sample. In this study, gradient surface characteristics of a virgin polystyrene sheet were produced via plasma treatment by control of exposure time. Surface characterization on the plasma treated specimens were conducted with contact angle measurement, scanning electron microscopy (SEM) and x-ray photo electron spectroscopy (XPS). Cell adhesion studies were also performed on gradient surfaces.

EXPERIMENTALS - The substrate polymer used for plasma treatment is a virgin polystyrene sheet (plate) of 0.09cm x 1.2cm x 4.5cm. The sheet was treated with a custom design plasma apparatus. The power supply was 220 Volt, 15 mA at 100 KHz. The treatment was performed in a constant oxygen pressure, 0.05 torr. A movable sample was mounted in the plasma reaction chamber to permit a controlled exposure of the sample to the plasma as shown in figure 1. A fixed mask was made of polystyrene. Sample has been translated using a motorized drive and exposed to the plasma up to 25 seconds. Contact angles of water were read every 2mm interval on the specimen. The attachment of Chinese hamster overy cell was conducted with routine procedures of the Toxicology Laboratory in KRICT. The amount of adhering cells were determined by counting the number of cells per 6 mm² of the of the substrate surface. XPS work is being conducted by University of Utah. Surface analysis was attempted by fourier transform infrared spectroscopy in the attenuated total reflectance mode (FTIR/ATR) using a spectrophotometer.

RESULTS - Figure 2 shows the average values of air water contact angle and cell adhesion on the surface of oxygen plasma discharged polystyrene as a function of the treatment time, respectively. The characteristics of wettability on the specimen were determined with the sessile drop method. The result shows that the wettability increased with increasing plasma exposure time. The gradient of contact angle in the plate was in a range of 88 to

35 degree. It was also observed that the number of cell adhesion per unit area in the plate shows a maximum value around 60 degree of the contact angle. SEM study (up to 50,000x) could not detect the difference of morphology between the treated and untreated ones. FTIR-ATR studies did not also show any difference between them.

REFRENCES 1. P.B. van Wachem, et al, Proceedings XI Annual Meeting ESAO, vol 2(1), 98, 1984. 2. H. Tanzawa, et al, Biomedical Polymers, E.P. Goldberg and A. Nakazima, eds, pp 189-211
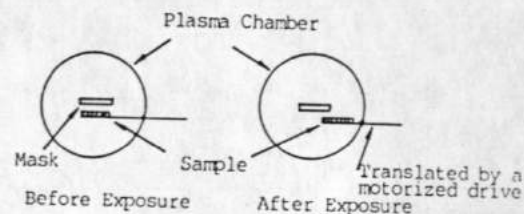
Figure 1. A movable sample was mounted in the plasma reaction chamber to controll exposure of the sample to the plasma environment.
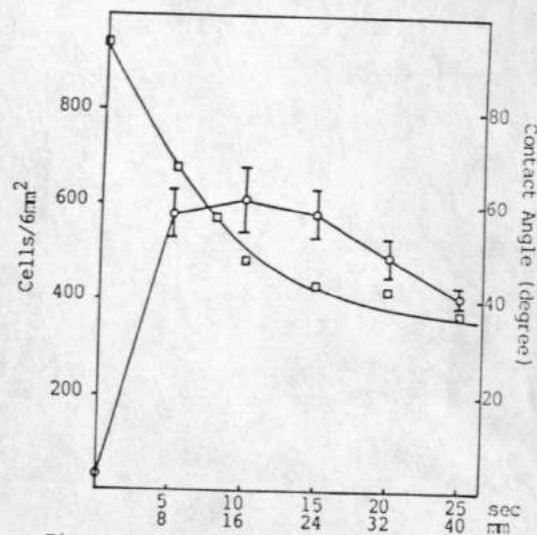

Figure 2. Contact angles (□) and numbers of cell attachment (o) on the gradient plate. The number of cell attachment plotted with the variation of plasma treatment time (sec) and the position from the distance on hydrophobic end (mm)

75-Word Abstract Form

(New Deadline—Extended Abstract must be submitted with the 75-Word Abstract by May 1, 1985)

Las Vegas, Nevada—October 13-18, 1985

Abstract No. ....
(to be assigned by the Society)

Schedule for ... Fiber Optics Sensors
(Title of Symposium)

Sponsored by ... Electronics/Luminescence and Display Materials
(Division/Group)

Title of paper ... Immunosensors Based on Evanescent-Excited Fluorescence

Authors (Underline name of author presenting paper.) ... <u>J-N Lin</u>, V. Hlady, W.M. Reichert, J.D. Andrade

Business affiliation and address ... Department of Bioengineering, College of Engineering

University of Utah

Salt Lake City, UT   84112   801-581-6911
(State or Country)   (ZIP Code)   (Telephone No.)

(Type abstract in this area—double-spaced.)

IMMUNOSENSORS BASED ON EVANESCENT-EXCITED FLUORESCENCE
<u>J-N Lin</u>, V. Hlady, W.M. Reichert and J.D. Andrade
Department of Bioengineering
University of Utah
Salt Lake City, Utah 84112

An electromagnetic field generated at a solid-liquid interface by total internal reflection optics is used to excite fluorescence of molecules present at the interface. Antibody (Ab) molecule immobilized at the surface of a quartz optical element bind their complementary antigen (Ag) from solution permitting analysis of antigen concentration in the bulk solution. The sensor can also be used to detect solution Ab by prior Ag immobilization. The Ab/Ag complex can be readily dissociated and the sensor reused. Sensing can be performed using the intrinsic ultraviolet fluorescence of the protein used or visible wavelengths using a fluorescent dye-labeled protein. The method is applicable in the fiber optic mode using a cladding-free fiber optic sensor. This work is supported in part by a grant from the Office of Naval Research.

Do you require any audiovisual equipment?

X 35 mm (2 x 2 in.) slide projector

☐ Vu-Graph

☐ other (specify)

Has the information in this abstract been presented verbally, submitted for publication, or published?
☐ Yes   X No
If the answer is yes, please provide the reference (except in the case of invited review presentations). _____

Is a full length paper on this work to be submitted for Society Journal publication?   ☐ Yes   X No

Charles Struck, GTE Labs

Immunosensors Based On Evanescent-Excited Fluorescence

J-N Lin, V. Hlady, W. M. Reichert, J. D. Andrade
Dept. of Bioengineering
College of Engineering
University of Utah
Salt Lake City, Utah 84112

Several groups have shown (1-5) that the evanescent wave generated at a solid-liquid interface by total internal reflection optics can be used to sense antigen (Ag)-antibody (Ab) reactions at the interface. We have applied this method to fundamental studies of protein adsorption at solid-liquid interfaces and to the development of optical sensors for Ag or Ab. (2,5-7).

The basic concept is given in Figure 1 below. Most proteins of interest are intrinsically fluorescent (excitation at 280/nm, emission at ~ 340/nm) due to the presence of tryptophan amino acids (6). Protein can also be readily covalently labeled with extrinsic fluors, such as fluorescein (excitation at 485/nm, emission at 515/nm), which provide higher quantum yields and increased sensitivity. The concept can be applied in single or multiple reflection modes, as well as using fiber optics (7) or thin film waveguides (8). These methods are being developed to produce truly remote, semicontinuous bio-specific sensors (5).

Figure 2 present typical data for the intrinsic UV experiment (no extrinsic labels used) described in Figure 1. Human IgG was preadsorbed onto a dimethyl-dichloro silane (DDS)-treated silica surface (which is highly hydrophobic). The IgG surface was exposed to increasing concentrations of anti-human IgG (from 0.05 to 1 mg/ml in phosphate-buffered saline). Even in the relatively insensitive UV mode, a respectable assay can be obtained (2).

Figure 3 demonstrates Ab detection (using fluorescein-labeled anti-human IgG) by binding to preadsorbed Ag, human-IgG.

Figure 4 shows Ag detection by binding to preimmobilized Ab. In this case the Ag is fluorescein-labeled human IgG. The Ab is anti-human-IgG and is covalently immobilized onto a glutaraldehyde-treated albumin monolayer on a DDS-quartz surface.

Both Figures 3 and 4 show the disruption of the Ab-Ag complex and demonstrate multiple use of the same sensor surface.

These data demonstrate the feasibility of evanescent-excited fluoroimmunoassay for the development of practical, remote, specific biosensors.

References

1. M. N. Kronick and W. A. Little, J. Immunol. Meth., 8 (1975) 235.
2. J. D. Andrade and R. A. Van Wagenen, U.S. Patent 4368047, Jan. 11, 1983.
3. T. Hirschfeld, U.S. Patent 4,447,546, May 8, 1984.
4. R. M. Sutherland, C. Dahne, J. F. Place, A. S. Ringrose, Clin. Chem. 30 (1984) 1533.
5. J. D. Andrade, R. A. Van Wagenen, D. E. Gregonis, K. Newby, J-N Lin, IEEE Trans. Elect. Dev., ED-32 (1985) in press.
6. V. Hlady, R. A. Van Wagenen, J. D. Andrade, Chapter in J. D. Andrade, ed., Interfacial Aspect of Biomedical Polymer, Vol 2., Protein Adsorption, Plenum Press, 1985.

7. K. Newby, W. M. Reichert, R. A. Van Wagenen, J. D. Andrade, Appl. Optics, 23 (1984) 1812.

8. W. M. Reichert, K. Newby, and J. D. Andrade, Trans. Soc. Biomaterials, 8 (1985).

FIGURE 1 Schematic of fluorescence signal as a function of time (top). Far left signals due to standards, center shows the adsorptive immobilization of antigen, right demonstrates binding of antibody from solution, resulting in a proportional increase in signal. Bottom idealizes the interfacial processes involved together with the total internal reflection and signal collection geometries.
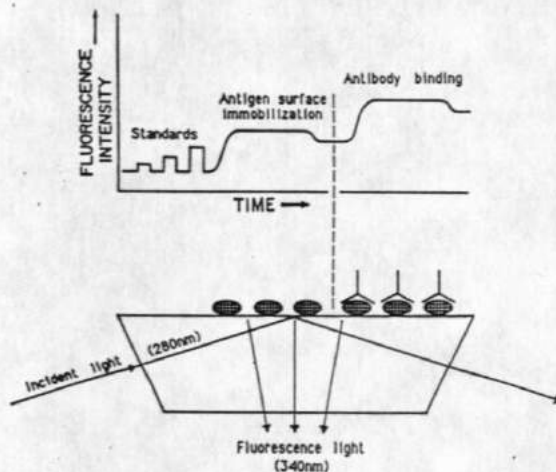
FIGURE 2 Intrinsic UV TIRF of human IgG preadsorbed on DDS-quartz and then exposed to increasing concentrations (0.05 to 1 mg/ml) of anti-human IgG. Even the relatively insensitive intrinsic UV mode is useful for quantitative immunosensing.
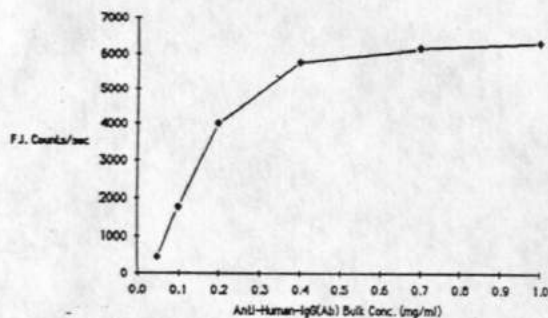
FIGURE 3 Bulk solution Ab detection by monitoring
extrinsic fluorescence of fluorescein-labeled IgG.
(a) PBS buffer background; (b) adsorption of
fluoroscein-Ag at the surface; (c) adsorbed signal
after PBS washout; (d) fluorescence quenched by
flushing with 0.01 M HCl pH 2 solution; (e) flushing
with PBS buffer; the difference between e and c
represents material desorbed by the acid treatment;
the e-d difference is due to acid quenching of the
irreversibly adsorbed Ab; (f), (g), and (h) are the
same as (b), (d), and (e), respectively, demonstrating
reproducibility; (i) injection of fluorescein-labeled
Ab; (j) flushing with PBS buffer; (k) disruption of
specific Ab-Ag binding by 0.01 M HCl pH 2 solution;
(l) flushing with PBS buffer; (m), (o), and (p) are
the same as (i), (k), and (l).
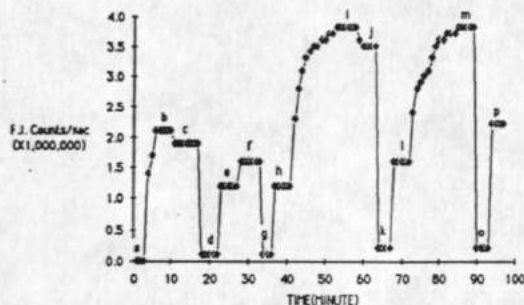
FIGURE 4 Specific binding of fluorescein-labeled
human-IgG(Ag) onto preimmobilized anti-human-
IgG(Ab). Original surface is glutaraldehyde-
crosslinked bovine serum albumin (BSA) on DDS-treated
silica. (a) PBS buffer background; (b) adsorption of
Ag at the Ab-covered surface; (c) removal of bulk Ag
solution by PBS flush, plateau represents Ag
irreversibly bound to Ab; (d) removal of Ag by
flushing with 0.01 M HCl pH 2 solution; (e) injection
of PBS buffer, the difference between c and e
represents Ag removed by 0.01 M HCl solution. The
difference between e and d is due to acid quenching of
the fluorescence of the irreversibly bound Ag; (f)
injection of BSA to check nonspecific adsorption; (g)
injection of PBS; the fact that e and g are identical
shows no adsorption of BSA, suggesting that the
surface is indeed saturated with the preimmobilized
Ab; (h)-(k) represent the same procedures as (a)-(e)
except that degree of Ag labeling at (h) is higher.
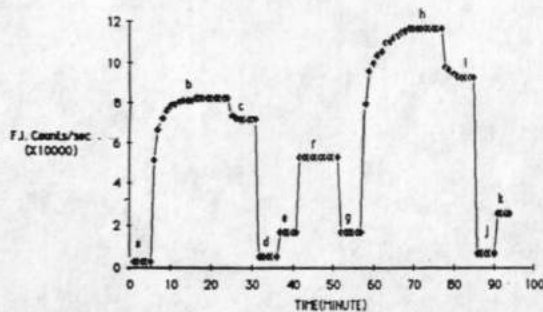
21.1

Ab—Ag INTERACTIONS ON SILICA SUBSTRATES FOR IMMUNOSENSORS
Lin, J.N., Herron, J.N., Kopecek, J., and Andrade, J.D.

Department of Bioengineering, University of Utah, Salt Lake
City, Utah 84112

An electromagnetic field generated at a solid-liquid interface by total internal reflection optics is used to excite fluorescence of molecules present at the interface. Antibody (Ab) molecules immobilized at the surface of a silica optical element bind their complementary antigen (Ag) from solution, permitting analysis of antigen concentration in the bulk solution. Ab in solution can also be detected by prior Ag immobilization to silica surfaces. Sensing can be performed using the intrinsic ultraviolet fluorescence of the proteins or by visible wavelengths using fluorescent dye-labeled proteins.

After showing the feasibility of sensing Ab-Ag interaction on silica substrates by total internal reflection, the radioimmunoassay technique was used to characterize the physical and chemical properties of immobilized Ab on three different pretreated silica surfaces. Two Ab-Ag model systems, goat anti-Human IgG Ab (polyclonal Ab)/Human IgG (multivalent Ag) and mouse anti-digoxin IgG (monoclonal Ab)/digoxin (monovalent Ag), were used. Both physical and covalent immobilization of Ab on silica surfaces were investigated. We will present data and analyses regarding: equilibrium binding constants of the Ab-Ag interaction, non-specific binding, maximum Ag binding capacity, surface concentration and stability of immobilized Ab, and the effect of immoblization time on Ab activity.

In order to maximize sensor sensitivity, it is disirable for the Ab-Ag constant to be as high as possible. Unfortunately, the specificity and high affinity of Abs also has a negative consequence--it is difficult to reversibly dissociate the Ab-Ag complex once it is formed. This problem is circumvented in the case of immunoassays by using reagents only once. One shot assays are adequate for routine diagnostic testing, but some environments require remote and /or continous testing, such as the immunosensor we are interested in. Therefore, in order to reuse such a device, there must be a means to weaken the bond to permit the complex to dissociate in a reasonable time. Several approaches are suggested based on photo-isomerization processes which change the microenvironment of the binding site, which in turn affects the binding constant. Some of preliminary data will be presented and discussed.

REMOTE, CONTINUOUS, MULTICHANNEL BIOCHEMICAL SENSORS BASED OF FLUOROIMMUNOASSAY TECHNOLOGIES

J-N Lin, P. Kopeckova*, J. Ives, H. Chuang, J. Kopecek*, J. Herron, H-R Yen, D. Christensen, J.D. Andrade
Department of Bioengineering
University of Utah
Salt Lake City, UT 84112, U.S.A.
*Institute for Macromolecular Chemistry
Prague 6, Czechoslovakia

The advances in fluoroimmunoassay, coupled with the rapid development of fiber optics, planar waveguides, and integrated optics, make it feasible to construct and apply remote, continuous multichannel biochemical sensors. The development of such immunosensors requires: a) preparation, characterization, selection, and immobilization of the needed antibodies or antibody fragments; b) a means to deliver remotely the fluor or fluorescently-labelled competing Ag; c) a means to regulate the Ag-Ab binding properties to allow reasonable response times or externally controlled "zeroing" of the sensor; d) an inexpensive and reliable means to excite fluorescence with minimal excitation of general background fluorescence; e) a convenient means of detecting, collecting, and processing the emitted fluorescence so as to obtain a quantitative assay; f) means to provide many sensing channels to permit the assay of 2 or more analytes together with the needed reference and blank channels.

We are addressing all of these problems in a coordinated fluorosensor development program. Progress on each of the component areas will be briefly discussed using results from prototype sensors for prothrombin and antithrombin III.

DISCUSSION

MEL SWANSON: You stated that for covalent immobilization to occur, an antibody has to adsorb first. Would that be true only of hydrophobic surfaces, or would it also be true of hydrophilic surfaces?

JOE ANDRADE: It's got to get there first, and it has to have a residence time there greater than a thermal fluctuation. And that means basically an adsorption event. That adsorption event and the covalent immobilization can occur almost simultaneously, but it's unlikely, because it's coming up to the surface.

There is a repertoire of functional groups on the surface of a protein – the amino groups that are used to covalently immobilize it (sulfhydryl, etc.) There is also a whole array of nonpolar groups on most protein surfaces – so-called hydrophobic patches. On a hydrophobic surface, the protein which is the most tightly adsorbed is certainly adsorbing through the face with the greatest hydrophobic character.

There's a whole variety of collision events and processes going on. You must imagine the protein interacting with the surface, colliding with that surface through all possible orientations. Some of those orientations essentially lead to no residence time or just diffusion-limited residence time. Other orientations lead to a substantial residence time. Those orientations are not necessarily the same orientations required for covalent immobilization. After the abdsorption event, the thing diffuses around on the surface and partially denatures. And in that squirming on the surface, which takes on the order of seconds to minutes to even longer, it finally finds a reactor group. And then the reactive event may occur. The adsorption event is critical to the immobilization event in most systems.

FIRST INTERNATIONAL SYMPOSIUM

FIELD SCREENING METHODS FOR HAZARDOUS WASTE SITE INVESTIGATIONS

October 11-13, 1988

Co-Sponsors
U.S. Environmental Protection Agency
U.S. Army Toxic and Hazardous Materials Agency

4C1-33 PHOTOREGULATION OF AB-AG AFFINITIES FOR IMMUNOSENSOR APPLICATIONS

J-N Lin, J. Herron, P. Kopeckova,* J. Kopecek,* and J.D. Andrade

Department of Bioengineering, College of Engineering, University of Utah
Salt Lake City, Utah 84112

There has been considerable interest in the use of optical fibers for remote spectroscopic sensing of biomolecules. The basic idea, in short, is to immobilize a receptor (e.g. antibody) on the surface of an optical element to specifically detect the ligand (e.g. antigen) in solution. Various sensing techniques have been developed by many groups. We are developing an immunosensor using an evanescent wave to excite fluorescence of molecules present at the interface. Fiber optic immunosensors should be fast, sensitive, specific, remote, and semicontinuous. The sensor must be designed to be reusable. In order to maximize sensitivity, it is desirable for the Ab-Ag constant to be as high as possible, meaning the off-rate is very slow--hence slow response times. Thus, in this study, we are looking for a means to "zero" the sensor between each measurement without sacrificing the sensitivity.

A panel of anti-fluorescyl monoclonal Abs and fluorescein Ag were used as a model system. Dianionic fluorescein is strongly fluorescent, but the fluorescence of Ab-bound fluorescein is quenched. Therefore, by
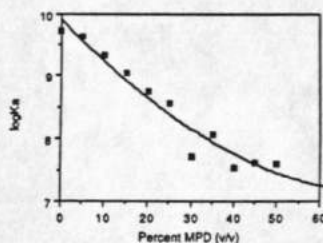

Figure 1: Effect of 2-Methyl-2,4-Pentanediol on the Affinity (Ka) of 4-4-20.

measuring the fluorescence intensity and polarization, the binding constant can be obtained. The thermodynamic properties of Ab-Ag binding in solutions were investigated. The solutions we have used include pH 8, potassium phosphate buffer (PPB), 2-methyl-2,4-pentanediol (MPD) in PPB, and N-(2-hydroxypropyl) methacrylamide (HPMA) in PPB. The results showed that the affinity of the anti-fluorescyl monoclonal antibodies is strongly dependent on the concentration of the solute (Fig. 1). It is believed that the decreased affinities are due to the decrease in conformational entropy of Ab because negative changes were observed in both ΔS° and ΔCp°. The temperature perturbation experiments also showed that ΔGu increased and the denaturation temperature decreased with increasing MPD concentrations (Fig. 2). By understanding the association and dissociation mechanism of Ab-Ag interaction in solutions, we proposed a method based on the photo-isomerization of copolymers which change the microenvironment of the Ab binding sites, and in turn affects the affinity.

The proposed copolymer has the general structure shown in Fig. 3. The A units provide a hydrophilic, inert polymeric carrier and also

can lower the affinity of Ab via their solute effect. The B units provide the photo-isomerizable azo groups. The C units provide the acid polyelectrolyte character needed for coil expansion and contraction. The D units provide a reactive group which can be used to bind the copolymers to Abs. We started with a copolymer containing B and C units to see the effects of azobenzene on carboxyl groups before and after irradiation by the light. A change in
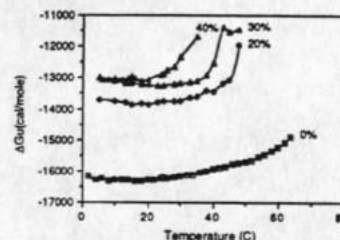
Figure 2: Unitary free energy (ΔGu) for the binding of fluorescein by monoclonal anti-fluorescyl Ab 4-4-20 in various concentrations of MPD.
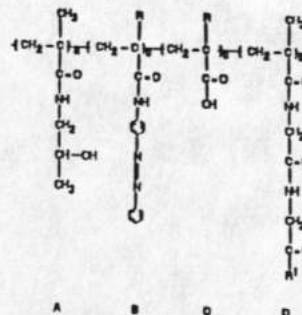
Figure 3: General structure of the proposed copolymer.

pH was observed. Two different methods for introducing the azobenzene side chain were compared. The kinetics of photo-isomerization were also studied. A series of compositions of azobenzene-containing copolymers were synthesized. The conformational changes of copolymers caused by photo-isomerization were investigated by measuring the viscosity and hydrodynamic diameter (light scattering) as a function of pH, temperature, and ionic strength.

REAL TIME IMAGING OF IMMUNOGLOBULIN ADSORPTION ON MICA USING THE ATOMIC FORCE MICROSCOPE

J.N. Lin, B. Drake[†], A.S. Lea, P.K. Hansma[†], and J.D. Andrade

Dept. of Bioengineering, Center for Biopolymers at Interfaces, University of Utah
Salt Lake City, Utah 84112 USA

Introduction

There are a number of methods to study the adsorption of proteins at interfaces including radiolabelling, scanning electron microscopy, and a variety of spectroscopic techniques. The problem with these methods is that it is not possible to image the molecular arrangement of adsorbed molecules, let alone individual molecules on a surface. Furthermore, some of these techniques can not monitor the adsorption events in real time or in an aqueous environment. The advent of the atomic force microscope (AFM) has enabled researchers to monitor real time processes in an aqueous environment. Recently, the AFM community at UCSB was able to image the adsorption and polymerization of fibrinogen on mica demonstrating the potential of the AFM for observing biological processes.[1]

With an invitation to use the AFM instrumentation at UCSB, those of us at Utah decided to study the adsorption of a monoclonal IgG (4-4-20) on mica.[2] This protein was chosen because it is easily crystallizable and was therefore expected to display non-random adsorption.

Methods

Mica was attached onto the piezoelectric crystal and a fresh surface was produced by cleaving in situ. A flow cell was erected around the mica and distilled water was introduced. The piezoelectric stage was advanced until the force between the AFM tip and the sample approximated 10^{-9} N. Images of the mica surface were thus obtained. After tip retraction, the distilled water was exchanged with an 18 mg/mL solution of IgG (4-4-20) in phosphate buffered saline (pH 7.4). Images obtained showed the progression of IgG adsorption dynamics. IgG desorption in distilled water was investigated as well.

Results and Discussion

Images were obtained in both feedback and variable force modes over a typical scan area of 4500 Å by 4500 Å. The image of the mica was featureless indicating a flat, virgin surface.

Images from the IgG solution experiment showed adsorption was a cooperative process. The first images were obtained in feedback mode and showed a growing IgG aggregate. The scan area here was 1800 Å by 1800 Å. After 5 minutes from the time of protein addition, the scan area was increased to 4500 Å by 4500 Å and 'ridges' appeared. The scanning mode was switched to variable force mode and the same image appeared. Rarely were isolated molecules seen and those that were observed disappeared by the next image (5 seconds later). Yet, those that landed adjacent to the ridges adhered resulting in growth in the plane of the surface. These observations indicate that lateral interactions are necessary for a stable protein layer on mica. The adsorbed layer continued to grow in two dimensions producing a near complete monolayer at 20 minutes. At 30 minutes, a second IgG layer depositing on the monolayer becomes visible. No desorption of the IgG layer in distilled water was observed, even after 10 minutes, perhaps due to the strength of lateral interactions.

Since individual IgG molecules were not observed in these images, we are now trying to obtain images of an easily crystallizable IgM pentamer. Due to its symmetry and larger size, we hope to be able to see individual molecules.

Image 1: Variable force mode image of 18 mg/mL IgG 4-4-20 in PBS adsorbing on mica after 5 1/2 minutes. Scan area is 4500 Å by 4500 Å. Note formation of 'ridges'.

Image 2: Variable force mode image of 18 mg/mL IgG 4-4-20 in PBS adsorbing on mica after 20 minutes. Scan area is 4500 Å by 4500 Å. A monolayer is nearing completion.

References:
1) B. Drake, C.B. Prater, A.L. Weisenhorn, S.A.C. Gould, T.R. Albrecht, C.F. Quate, D.S. Cannell, H.G. Hansma, P.K. Hansma, Science 243 1586 (1989).
2) J.N. Lin, B. Drake, A.S. Lea, P.K. Hansma, J.D. Andrade, Langmuir, submitted for publication Sept. 1989.
3) A.L. Gibson, J. N. Herron, X.M. He, V.A. Patrick, M.L. Mason, J.N. Lin, D.M. Kranz, E.W. Voss, Jr., A.B. Edmundson, Proteins 3 155 (1988).

†Dept. of Physics, University of California
Santa Barbara, California 93106 USA

MONDAY

OBSERVATIONS OF VON WILLEBRAND FACTOR DEPOSITED ON MICA AND IMAGED BY ATOMIC FORCE MICROSCOPY

R.E. Marchant, A.S. Lea[1], J.D. Andrade[1], P. Brockenstedt[2] and D. Ginsberg[2]

Department of Biomedical Engineering, Case Western Reserve University
Cleveland, Ohio 44106

INTRODUCTION

Interactions of plasma proteins with surfaces are extremely important phenomena that affect bioadhesion events in many physiologic and pathologic processes including thrombosis formation on biomedical polymers and other biomaterials. Analysis or modeling of this behavior is inherently complicated by a wide range of potential protein interactions. If these factors are coupled with the substantial heterogeneity of biomedical polymer surfaces, it is not surprising that progress in understanding the initial events of thrombosis formation has been slow. In particular, there is only limited fundamental appreciation at the molecular level, of the interactions of plasma proteins at solid/liquid interfaces. However, direct investigations of protein-surface interactions are now feasible by using the experimental techniques of atomic force microscopy (AFM) and scanning tunneling microscopy. AFM has been used by others to obtain nanometer resolution images of both conductors and non-conductors, including molecules of polyalanine, and of thrombin-activated polymerization of fibrinogen to fibrin polymer. In our studies, we have used AFM to obtain molecular level images of von Willebrand factor (vWF). VWF is of considerable clinical importance, as well as having a potentially crucial role in thrombus formation on biomaterials. VWF is a plasma glycoprotein that mediates adhesion of platelets to substrata such as subendothelium and possibly biomaterials, and acts as a carrier molecule for the coagulation protein factor VIII. VWF exists in the circulation as large disulfide-linked multimers, ranging in molecular weight from 0.5 to 20 million Daltons. VWF has been visualized previously by TEM as an elongated, flexible molecular filament of varying lengths, typically 60 nm to over 1100 nm fully extended. The large size of vWF and its relevance to blood-materials interactions made it an attractive molecule for preliminary investigations by AFM.

METHODS

Purified human vWF was prepared from cryoprecipitate and separated from Factor VIII at the University of Michigan, according to previously published methods. Purified vWF in TBS-azide buffer (10mM Tris, pH 7.5, 140 mM NaCl, 0.02% sodium azide) was stored at -20°C. AFM images of human vWF were obtained using a Digital Instruments Nanoscope II. Atomic resolution images of the freshly-cleaved, atomically-flat mica surface were obtained before imaging vWF. Samples were prepared for AFM imaging by depositing a 2 uL aliquot of vWF (0.4 or 0.04 mg/mL) on the freshly cleaved mica. The samples were then dried in air and imaged by AFM within 1-2 h. VWF samples were removed from the piezoelectric stage, rinsed thoroughly with distilled water and re-imaged after drying in air for over 5h. AFM Images (400 x 400 data pixel density) were obtained in both constant force and constant height modes over scan areas of 0.1 to 10 microns.
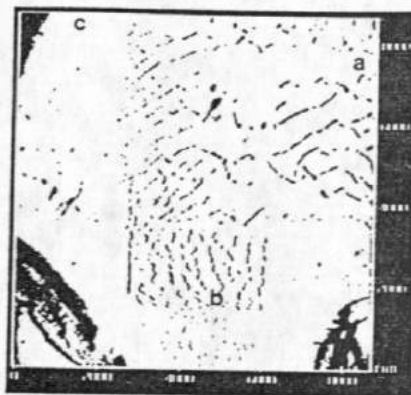
RESULTS AND DISCUSSION

The ability to obtain three dimensional images of proteins on surfaces by AFM depends on the interactive forces between the two-dimensional solid surface and the protein, relative to the tracking force (approx. 1 to 10 nN) applied to the protein by the cantilever tip. If the tracking force is greater than the surface-protein adhesive force then the protein will be "moved" by the probe tip. This phenomenon was observed for vWF deposited on mica. Thus, vWF molecular aggregates 40 nm thick (width dimension) seen in a 1.3 x 1.3 micron three dimensional image, became 100 nm thick vWF molecular aggregates in the following image. Continued imaging caused further aggregation of the vWF molecules. This effect of protein "manipulation" was illustrated dramatically, when the probed area was viewed at a higher scan area (8 x 8 micron) and scan rate. This is shown in the figure. Area 'a' has been scanned repeatedly, area 'b' was scanned 2-3 times and area 'c' shows a relatively undisturbed layer of vWF. In contrast, AFM images of vWF obtained after rinsing the samples and re-imaging showed individual vWF molecules adsorbed on the mica, that were not perturbed by the tracking force applied by the cantilever tip. From scan areas of 200 x 200 nm to 1 x 1 micron, individual vWF molecules were observed. As in previous TEM studies, VWF molecules observed by AFM covered a wide range of dimensions. The largest "individual molecules" observed were up to 800 nm in the longest dimension, but molecular sizes in the order of 100 nm to 400 nm were most common with measurements of 2 to 4 nm in the 'z' direction. These preliminary studies have shown that three dimensional molecular level images of protein molecules such vWF can be obtained using AFM. However, in these studies, it would be unreasonable to assume that the strongly adsorbed and air-dried vWF molecules are in "native" conformations.

[1] Center for Biopolymers at Interfaces, University of Utah, Salt Lake City, Utah 84112.
[2] Medical Sciences Research Institute, University of Michigan, Ann Arbor, MI 48109.

Towards the development of a multi-analyte kidney chip to measure metabolites related to renal failure

Praveena Mohan, Joseph Andrade
Department of Bioengineering, University of Utah

PURPOSE

The objective is to create bioluminescence and chemiluminescence assays to measure metabolites relevant to the management of chronic renal failure. Renal chip will be a single use disposable device, similar in ease of use to a modern glucose meter and glucose test trips (1). It will be a multi analyte chip that can be used to measure metabolites related to the chronic renal failure. The analytes chosen are glucose, creatinine, urea and phosphate which are essential to monitor kidney function. Only the assay development is studied here. The chip and the optical device to measure light are being developed by others in our group. For these assays to be effective in a renal chip, the assays have to be sensitive so that only small amount of sample (blood/urine) is needed; enzymatic luminescence reaction is very sensitive and therefore only micro and nano volumes of sample are required. Assays must provide a useful calibration curve covering the concentration range needed for each analyte. The methodology for this is described here specific to creatinine.

INTRODUCTION

There are two ways to measure an analyte, either through production assay or competitive assay. Two luminescence platforms have been used for the above mentioned objective. They are; Chemiluminescence using Luminol and Bioluminescence using Firefly luciferase (2,3).

This luminescence reaction can be either coupled to metabolite involved reactions that produce or consume H_2O_2 or reactions that produce or consume ATP. Therefore, the measured light intensity will be directly proportional to the concentration of metabolite.

PRODUCTION ASSAY

Analyte + Reactants H_2O_2 or Analyte + H_2O_2 Products

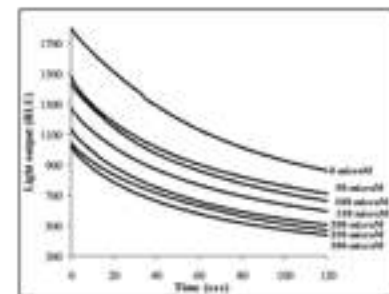**Horse Radish Peroxidase**
Luminol + H_2O_2 3-aminopthalate + Nitrogen + 2 Water + Light
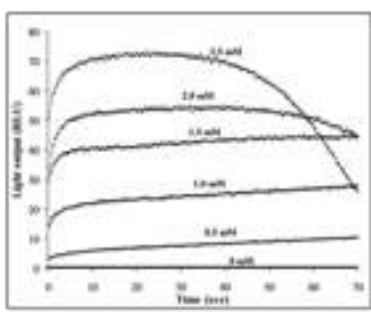
COMPETITIVE ASSAY

Analyte + **ATP**   product or Analyte + **reactant**   **ATP**

Firefly Luciferase
Luciferin + Oxygen + **ATP**   Oxyluciferin + AMP + Pyrophosphate + Carbon dioxide + Light

Calibration curve

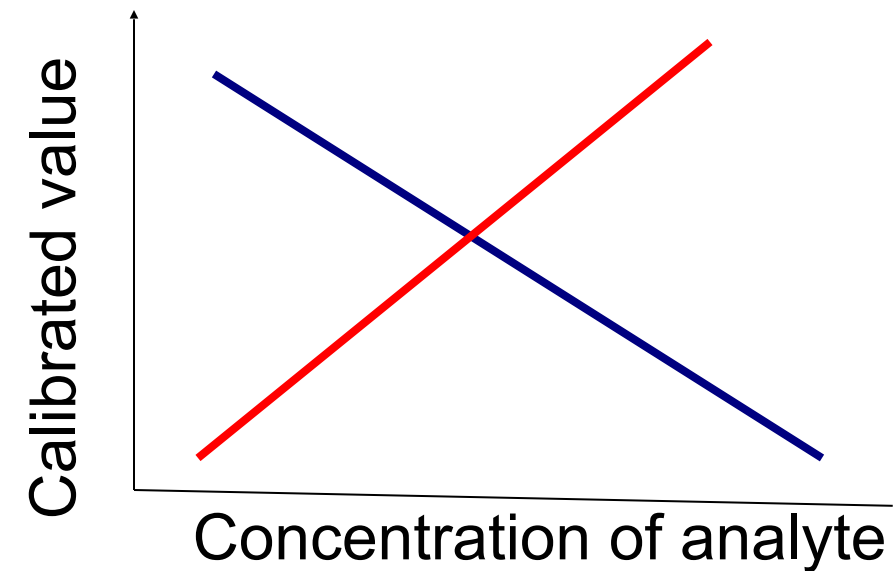Calibrated value

Concentration of analyte

Figure 1: Two different assays, productive and competitive assays are shown here with examples of how the output would vary with time with respect to concentration of metabolite

Creatinine was measured with firefly luciferase platform using a competitive assay (Figure 2). In this assay, creatininase converts creatinine to creatine. Creatine kinase then converts creatine to creatine phosphate using ATP. Since both reactions compete for ATP, higher the concentration of creatinine, lower the light output. MgSO4 was used since luciferase requires Mg^{2+} as cofactor for the luminescence reaction to proceed.
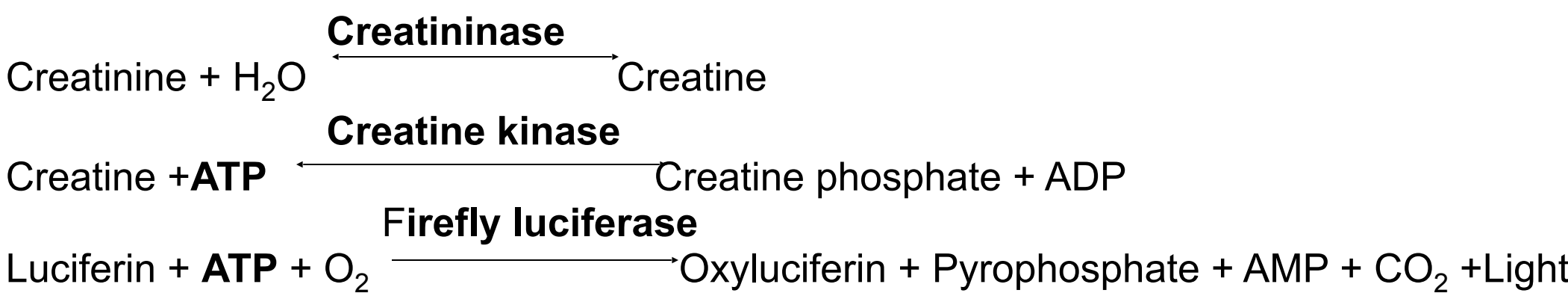
Creatininase
Creatinine + H_2O Creatine

Creatine kinase
Creatine + **ATP**   Creatine phosphate + ADP

Firefly luciferase
Luciferin + **ATP** + O_2 Oxyluciferin + Pyrophosphate + AMP + CO_2 + Light

Figure 2: Creatinine assay involves creatininase and creatine kinase reactions coupled with firefly luciferase reaction

METHOD

Different stages were involved in an assay development;

• Assay study and model
This reaction was modeled using a mass balance analysis. Using Matlab, these differential equations were solved and time versus reaction rate was plotted (Figure 3). Rate of the reaction is the number of moles of product formed per second (moles/s) and in our assay; it is the amount of light produced in the second reaction. The initial concentrations of creatinine used were 0, 50, 100, 150, 200, 250 and 300 μM.

• Choosing normalization technique – Z-Score
Model of the creatinine assay was chosen to demonstrate the feasibility of using Z-Score as a normalization technique. Rate (moles/s) data was normalized by Z-Score method.Z-Score indicates the standard deviations away from the mean of a specific observation. If the observation is X, from a population with mean μ and standard deviation σ, then
       Z= (X - μ) / σ
It is a simple statistical normalization method to compare different sets of data.
For all of these assays, area under the normalized curve (Z-Score curve – plot of time versus Z-Score) was the best since the normalized curve were almost horizontal lines (Figure 4,5).

• Testing of wet assay
Cocktail of all the reagents were prepared with ATP/MgSO4 prepared separately. 8.3 µL of cocktail was added to the luminometer tube and then 1.7 µL of ATP/MgSO4 was added. The luminescence reaction starts once ATP is added. After 30 s, 2.5 µL of analyte is added and luminometer is started. Time vs. light output data was collected. Calibration curve for the wet assay was obtained (Figure 6).

• Testing of wet assay in serum
The analyte (creatinine) was spiked in serum to determine whether similar results can be obtained (Figure 7).

• Testing of dry assay
Enzymes used in these assays are heat sensitive and therefore require freeze drying. Freeze drying can cause freezing and drying stresses (low temperature stress, formation of ice crystals, increase in ionic strength, pH change etc.,) that can denature the enzymes. Therefore excipients are added to stabilize the enzymes during freeze drying (2,3) (Figure 8,9).

Table 1: Rationale for using the following excipients in the dry assay

Excipient	Rationale
Bovine Serum Albumin (BSA) Poly Ethylene Glycol (PEG)	Polymers that act as both cryo and lyoprotectants. Stabilization is attributed to preferential exclusion, surface activity and hindrance of protein-protein interactions.
Glutathione (GSH)	Antioxidant
Sugar (Sucrose, Trehalose)	Acts as both cryo and lyoprotectant

RESULTS

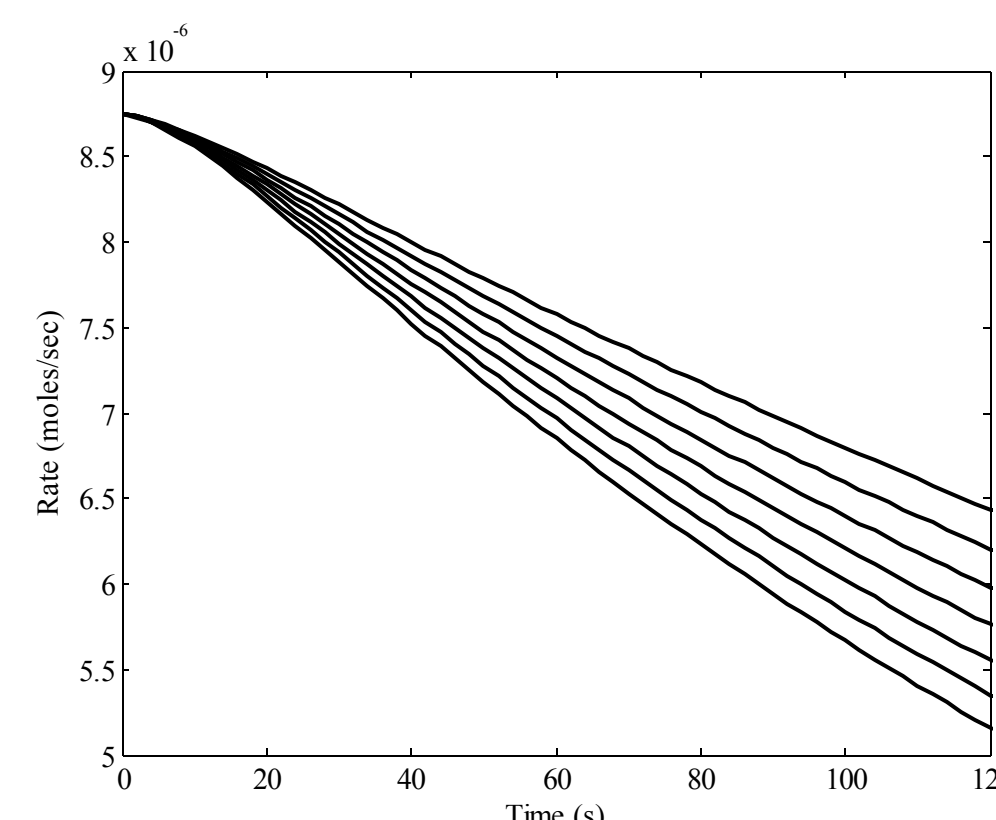• Assay study, model and understanding the normalization technique

Figure 3: Model of creatinine assay for different initial creatinine concentrations of 0, 50, 100, 150, 200, 250 and 300 µM. Rate is given by number of moles of product formed per second
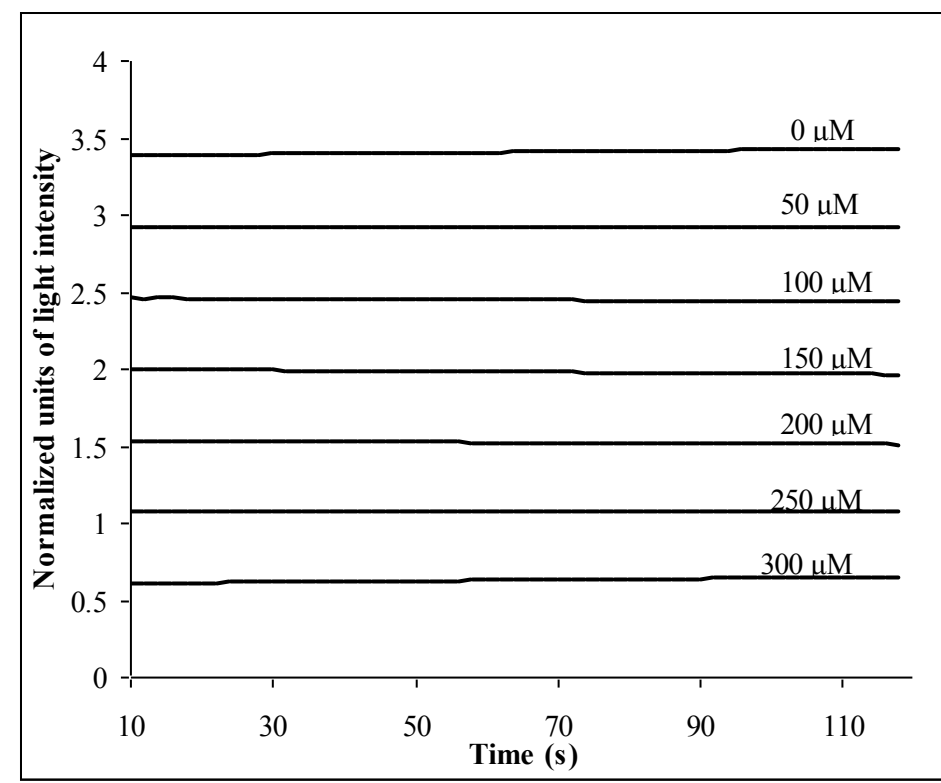
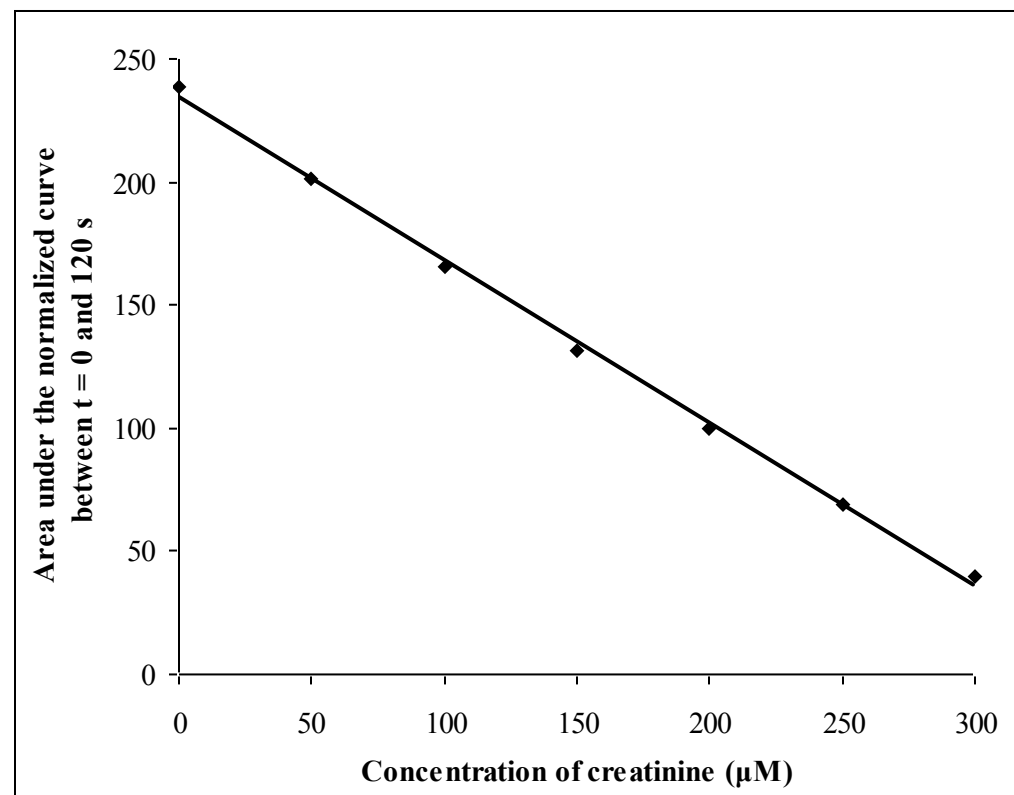Figure 4: Normalized data of creatinine model using Z-Score method

Figure 5: Calibration curve for the creatinine model using a linear fit

The calibration curve obtained for the model was a linear fit and also, it was clear that this normalization technique can be used for all of the assays to obtain a useful calibration curve.

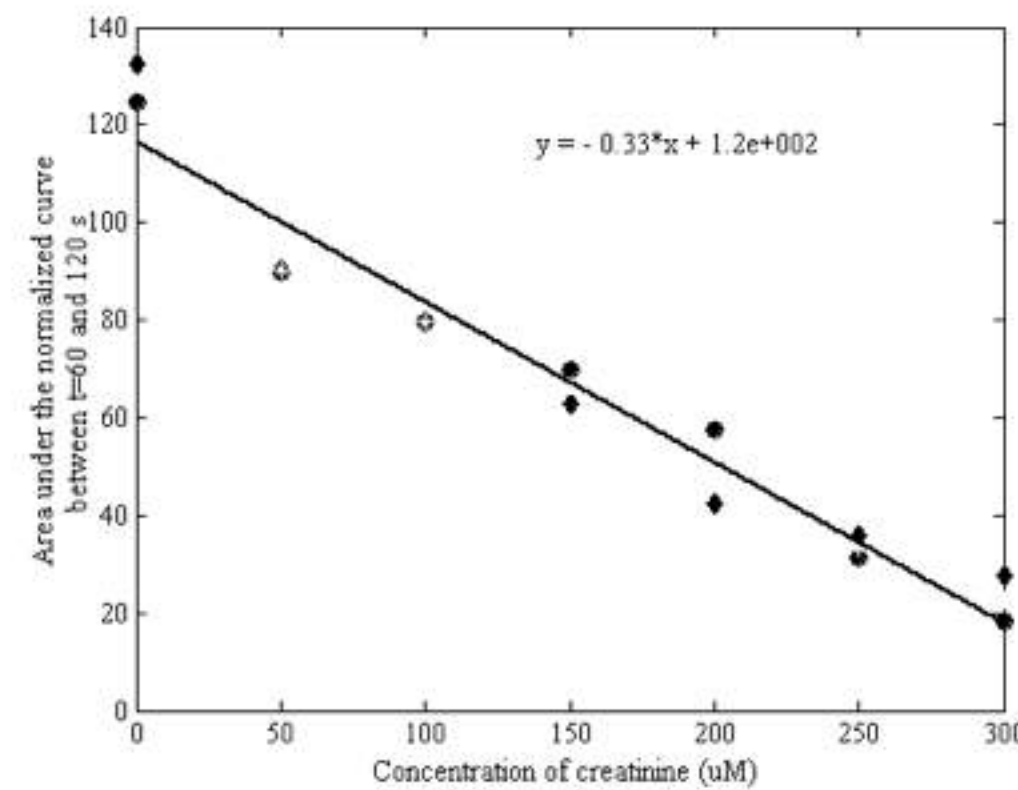• Testing of wet assay in buffer and serum

Figure 6: Calibration curve for the wet creatinine assay. The curve drawn is average of two sets of data (shown as circle and diamond) and represents the area under the normalized curve of time versus light intensity (RLU) (60-120 s). The average data (star) was fit with linear fit using Matlab fitting tool.
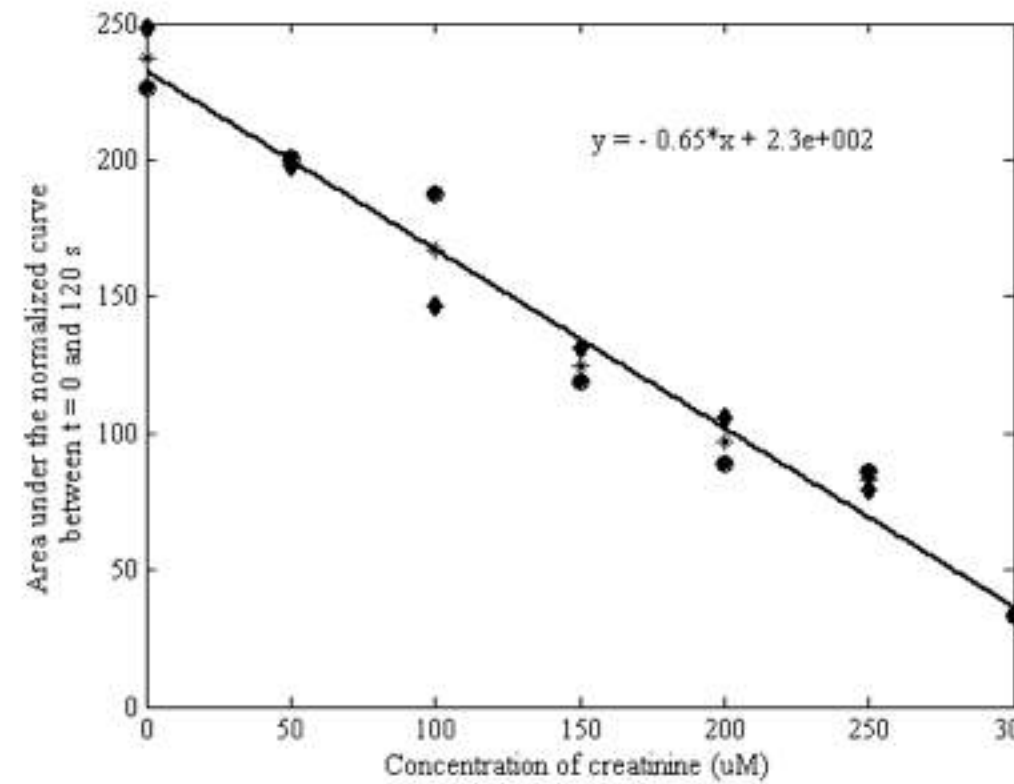
Figure 7: Calibration curve for creatinine assay with spiked concentrations of 0, 50, 100, 150, 200, 250 and 300 µM creatinine in serum. The average data was fit with linear fit using Matlab fitting tool. The sensitivity of the assay is approximately 0.7 units/microM concentration of creatinine except for the range 200 -250 microM where the calibration curves off.

When the assay calibration curves were compared with assays tested in buffer, both the calibration curves of creatinine assay were found to be almost similar with a small change in slope
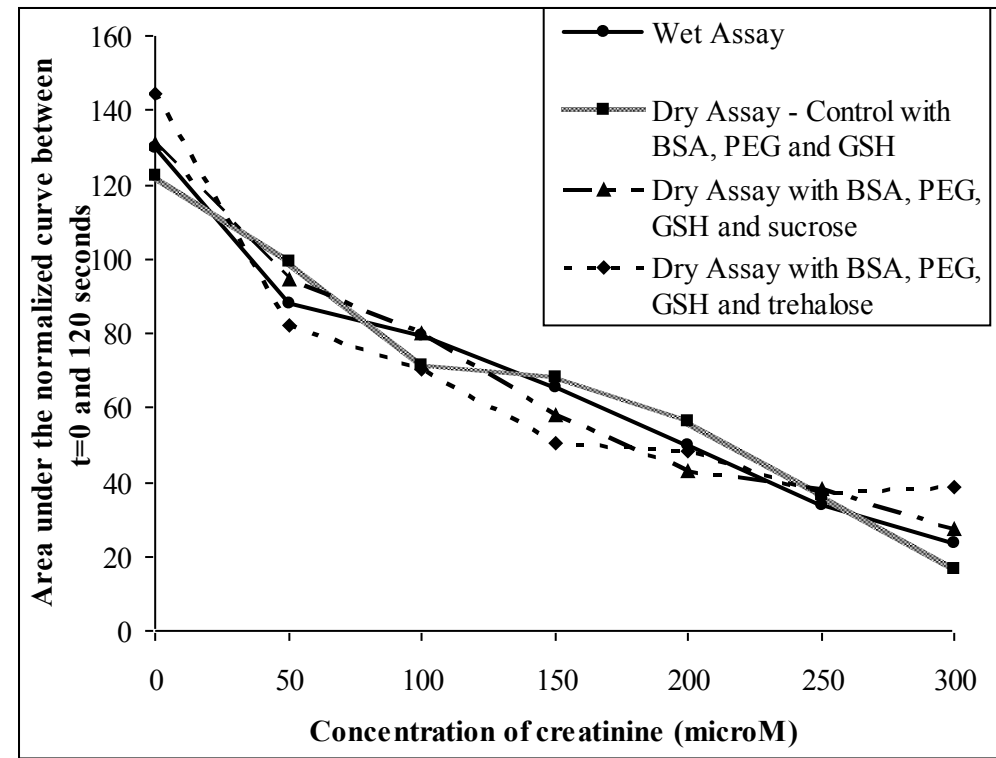
• Testing of dry assay

Figure 8: Comparison of calibration curves of wet assay, wet, dry assay + BSA + GSH + PEG and dry assay + BSA + GSH + PEG + sugar (sucrose and trehalose) for measurement of creatinine. All the data points are averaged from two/three data sets which are not shown here.
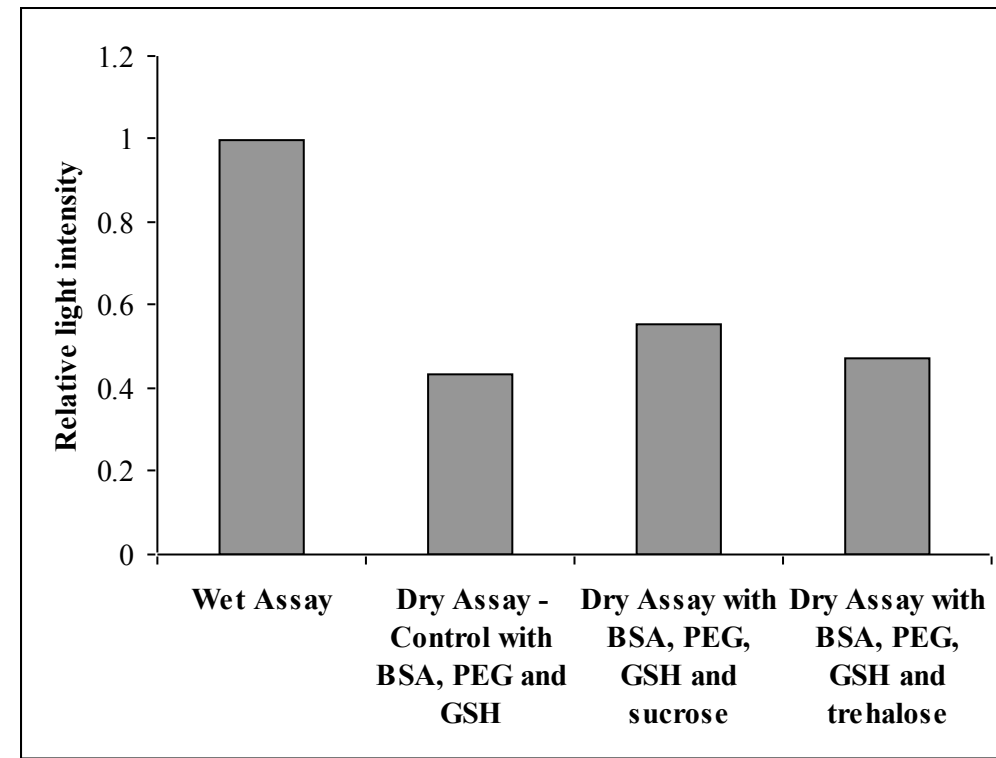
Figure 9: Comparison of increase/change in light output due to addition of different excipients as well as change in output before and after lyophilization for creatinine assay. Relative light intensity is the ratio of individual assay intensity to the maximum intensity among these five different assays such that they are standardized.

Dry assay control was only 44% of the wet assay output. After adding sucrose, the dry assay light output increased to 57% of the wet assay output.

DISCUSSION

This study revolved around the basic understanding of the assay, testing them in solution to determine the feasibility of the assay. The assays were modeled to understand the assay and to determine the best data analysis method using creatinine assay as an example. Cocktail was prepared, tested with different concentrations and the light output obtained was plotted against time for different analyte concentrations. The data was normalized using Z-Score method and area under the normalized curve was obtained and plotted against analyte concentration. Calibration curves were obtained for all analytes. The calibration curves were analyzed and found to be feasible.

These assays were studied in serum; and it was found that creatinine and urea assay tested in serum were very similar to the wet assay. For the other two assays, the calibration curves were different. Therefore there must be some interference in serum which needs to be further studied.

The assays were lyophilized and tested in dry form as similar to wet assay after reconstituting the dry assay with 10 µL of water. The output reduced due to decrease in enzyme. Therefore excipients were added to reduce the effect of lyophiliztion stress on the enzymes. Calibration curves were obtained for different excipients and compared. The best excipient for each assay was determined. Even though statistical significance of the data collected is not dealt in detail, this study will act as a ground work for future development of multi-analyte assays on a chip.

Future work will involve repeating the assays to test the reliability of the assay. More stabilizing agents need to be tested for better conservation of enzyme activity after freeze drying.

REFERENCE

1.Davies, R., Bartholomeusz, D.A., Andrade, J., "Personal Sensors for the Diagnosis and Management of Metabolic Disorders" IEEE engineering in medicine & Biology Jan/Feb2003: 32-42
2.Merenyi, G., J. Lind, et al., "Luminol chemiluminescence: chemistry, excitation, emitter." J Biolumin Chemilumin, 1990. 5(1): 53-62
3.Deluca, M., "Firefly luciferase" Adv Enzymol Relat Areas Mol Biol, 1976. 44: 37-68
4. Arakawa, T., Prestrelski, S. J., Kenney, W. C., Carpenter, J. F., "Factors affecting short-term and long-term stabilities of proteins" Adv Drug Deliv Rev. 2001 Mar 1;46(1-3):307-26
5. Wang, W., " Lyophilization and development of solid protein pharmaceuticals" International Journal of Pharmaceutics, 2000. 2-3; p 1-60

INSULIN AGGREGATION AND

ADSORPTION

by

Reed Donaldson Quinn

A thesis submitted to the faculty of
The University of Utah
in partial fulfillment of the requirements for the degree of

Master of Science

Department of Bioengineering

The University of Utah

December 1981

ABSTRACT

The solution and interfacial properties of the hormone insulin are important in the treatment of insulin deficiency diseases. The aggregation and adsorption characteristics of this molecule represent a major obstacle in the development of long-term insulin delivery devices. In addition, the small size of this molecule and the affinity with which it binds to the insulin receptor makes it an excellent model protein for the study of protein adsorption at the solid-liquid interface.

The purpose of this thesis is to outline the parameters that may affect insulin solubility and aggregation in aqueous solutions. It will also examine possible solution additives that may minimize insulin aggregation and improve the solubility without altering the molecular structure. Once these parameters have been established, a study of the adsorption characteristics of the molecule will be undertaken. Quantitation of the amount of insulin adsorption to various solid surfaces will be done using classical radio labelled and new total internal reflection fluorescence (TIRF) spectroscopy techniques.

The data presented here suggests that lysine, aspartic acid or glutamic acid may minimize insulin aggregation while

improving solubility. The results of radiolabelling and TIRF studies suggest the following conclusions:

1. Quantitation of insulin adsorption using the intrinsic tyrosine fluorescence is possible.

2. A close correlation between the two methods was observed.

3. A hydrophobic silanized glass and a silanized quartz surface appear to adsorb significantly more insulin than the corresponding hydrophilic unsilanized surface.

4. There appears to be a relationship between the amount of insulin adsorbed and the presence or absence of lysine in the protein solution.

of the obvious need at present there exists almost no litera-
ture in which the error induced by these approximations has
been studied. The main objective of this study is to provide a
step towards fulfilling this need.

We have studied here the three most important quantities
in a mathematical program, namely, the optimum objective
value, the optimum solution and the optimum dual solution.
We have quantified the extent to which these quantities of an
original program can deviate from the corresponding quanti-
ties which are obtained by solving its piecewise linear approx-
imation. This provides us with a measure to evaluate the
quality of an approximation by giving an idea of what possible
errors the approximation can make in estimating the relevant
quantities of the original problem.

Order No. 74-29,670, 134 pages.

ENGINEERING, MATERIALS SCIENCE

INVESTIGATION OF MICROSEGREGATION DURING
SINTERING OF A BINARY ALLOY

MISHRA, Amarendra, Ph.D.
Rensselaer Polytechnic Institute, 1974

Supervisor: F. V. Lenel

In this investigation microsegregation during sintering of
binary alloys has been studied with the help of an electronmi-
croprobe. Established concepts and previous work in this field
have been critically examined and compared with the experi-
mental results obtained from this investigation.

Homogeneous, 12 wt. % gold and silver alloy wires, 20 mils
in diameter were sintered at 740°C, 802°C and 849°C for differ-
ent lengths of time. The cross section of the neck between the
wires was examined with the help of an electronmicroprobe
to determine the concentration at different points in and adja-
cent to the neck. From the concentration profile it was con-
cluded that the initial neck growth as well as segregation takes
place by surface diffusion and that back diffusion (which causes
homogenization) occurs by a combination of surface and vol-
ume diffusion. With increasing time, volume diffusion becomes
more important. Grainboundary diffusion is not an important
mechanism for material transport during the period over which
segregation takes place. The highest enrichment observed
was 4% silver at the apex of the neck where the chemical po-
tential gradient due to a stress gradient is the highest. Silver
depleted regions were observed in only one sample sintered at
740°C for 10 minutes. Also the distance of these depletion re-
gions from the neck was 2 to 3 times the theoretically pre-
dicted distance. This has been explained on the basis of Hun-
tington's analysis which considers surface diffusion to be the
predominant mechanism for material transport during segre-
gation. This analysis applies to wires and is therefore appli-
cable to our experiments.

It has been established that existing theories have been
oversimplified or are not really applicable to microsegrega-
tion during initial sintering of alloys. Kuczynski's analysis
assumes that the mechanisms for segregation and homogeniza-
tion are the same, which has been shown to be incorrect by
our experiments.

In general, direct measurements of segregation have been
made rather than rely on the indirect methods, like precipita-
tion of a second phase, as done in the past. Definite conclu-
sions have been drawn with regard to the mechanisms respon-
sible for segregation.   Order No. 75-5390, 152 pages.

CHELATING POLYMERIC MATERIALS

RAMIREZ, Rene Santiago, Ph.D.
University of Utah, 1974

Chairman: Joseph D. Andrade

Accidental poisonings account for over fifty percent of
children's accidents. Present procedures of poisoning treat-
ment are of low effectiveness in certain severe cases or may
not be applied to small children. There is a need to improve
the emergency treatment of poisonings, particularly to de-
crease the period of coma and to minimize mortality.

Iron poisoning is a very common cause of poisoning among
young children. Use of chelating agents, especially deferox-
amine B, to remove excess iron from the body is one of the
most effective treatments. However, in very severe cases of
acute iron overload, the amount of deferoxamine to be given to
the patient to remove the iron would be so high that the drug
and its iron chelate become toxic.

Therefore, my objective was to develop a chelating polymer
to be used in extracorporeal detoxification of severe acute iron
poisoning cases.

Chelating polymers were prepared by grafting deferoxamine
B to the following polymers through covalent bond formation:
polyacrolein, poly(acrylyl chloride-co-styrene), poly(meth-
acrylyl chloride-co-styrene), poly(methacrylyl chloride-co-
styrene-co-vinyl pyrrolidone), chloromethylated polystyrene,
and chloromethylated polystyrene-divinyl benzene beads.

The characterization done on the precursor and chelating
polymers included elemental analysis, infrared spectra, den-
sity, viscosity, transition temperature, and solubility charac-
teristics. Stability and iron chelation characteristics were
studied in the chelating polymers.

The stability of the chelating polymers was determined in
saline solutions and in blood plasma by the amount of deferox-
amine liberated. The amount of deferoxamine liberated in both
normal saline and phosphate buffered saline of pH 7.4, after
seven days of contact, ranged from about 5×10^{-4} to 7×10^{-2}
grams of deferoxamine per gram of polymer or about 0.2 to
8.9% by weight of the deferoxamine bound. The lowest value
corresponded to the polystyrene-divinyl benzene-deferoxamine
grafts and the highest to that of polyacrolein-deferoxamine
graft. The stability in plasma could not be accurately deter-
mined. However, in all cases the deferoxamine liberated was
less than 5×10^{-2} grams per gram of polymer.

The experimental iron chelation capacity found for the poly-
mers ranged from 6.0 mg of Fe/g resin for the polystyrene-
divinyl benzene resins to 18.8 mg of Fe/g resin for the poly-
acrolein-deferoxamine resin. However, the efficiency, i.e.,
the ratio between the experimentally found capacity and the
calculated iron capacity of the resin ranged from 31% for the
polystyrene-deferoxamine graft to 44% for the poly(methacrylyl
chloride-co-styrene)-deferoxamine graft.

The stability constants and the distribution coefficients of
the iron complexes of the polymer-deferoxamine grafts were
determined from the iron content of the solid complexes and
the iron that they liberated into solution. The values obtained
for the stability constants were from 10^4 ℓ/mole for the poly-
styrene-divinyl benzene-based resins to 10^6 ℓ/mole for that
resin derived from poly(methacrylyl chloride-co-styrene).
The distribution coefficients ranged from 8 for the polystyrene-
divinyl benzene-based resin to 64 for the one derived from
poly(methacrylyl chloride-co-styrene).

The stability constants and distribution coefficients of poly-
mer-deferoxamine graft complexes with other ions (Ca, Mg
and Cu) were also determined. The values were lower than
those for iron, indicating a higher selectivity for the latter
metal.

One of these resins, that derived from Amberlite XAD-4,

was selected as a model to study the effect of initial iron concentration and amount of resin on the rate of iron chelation. A stirred batch system was used for iron in aqueous solutions and in plasma. In both cases the rate at which iron is removed was approximately the same for different initial iron concentrations ([Fe]$_0$) during the first hours of experiment. However, the time required to reach a constant iron concentration ("leveling-off time") increased with increasing [Fe]$_0$. The percent of iron removed was approximately the same (72-78%) for the various values of [Fe]$_0$ in aqueous solutions, but increased with [Fe]$_0$ for plasma medium.

The effect of varying the amount of resin was to increase the rate of iron removal as well as the amount of iron removed, and to decrease the "leveling-off time" in both water and plasma. In both media the percent of iron removed increased with increasing amounts of resin.

Column perfusion experiments done with iron in plasma showed an increase in the iron removal with respect to the removal obtained in batch experiments. Both variables [Fe]$_0$ and [R] had the same effect on the rate of iron removal as in batch experiments.   Order No. 75-7000, 172 pages.

METALLURGICAL ASPECTS AND MAGNETIC CHARAC-TERISTICS OF Sm-Co-Cu TERNARY SYSTEM

RIM, Chang, Ph.D.
University of Southern California, 1974

Chairman: Professor Y. B. Kim

The Sm$_2$(CoCu)$_{17}$ system has been studied to seek a better understanding of the interrelationships existing between the metallurgical structures and ferromagnetic properties, particularly coercivity. Comparison of the bulk and powder coercivity of annealed specimens indicates that the phase boundary is a nucleation center for reverse domain creation when the magnetization is reversed. This is verified by the direct observation of domain creation and growth at phase boundaries in a magnetization experiment.

In the cast material, on the other hand, the coercivity is largely influenced by domain wall pinning at the grown-in dislocation site. This conclusion is derived indirectly from the observed variation in microhardness in relation to the extrinsic and intrinsic magnetic parameters.
                    Order No. 75-6440, 131 pages.

ENGINEERING, MECHANICAL

ANALYSIS AND SYNTHESIS OF A MULTIPLE BELT AD-JUSTABLE VEE SIZE GRADER FOR SWEET POTATOES

BRANTLEY, Stanley Aurelius, Jr., Ph.D.
North Carolina State University at Raleigh, 1974

Supervisors: Donald D. Hamann and John K. Whitfield

A multiple belt, adjustable vee size grader was designed and developed for use in stationary sweet potato packing line applications. Product was graded by the machine on the basis of diameter. The machine incorporated 5 open bottom vees with ch vee side formed by 3 round 1/2 in diameter polyurethane ts. The bottom 2 belts (sizing belts) in each vee were used to size the product on a pass — no pass basis between the belts.

The distance between these 2 belts was adjustable. Prior to sizing, the longitudinal product axis had to be aligned with the sizing belt axes. The middle and upper belts (orienting belts which formed each side of the vee were individually driven to create a differential speed relationship across the vee. Product which was skew with respect to the belt axes and came in contact with orienting belts on both sides of the vee was turned until it was sufficiently aligned to roll to the bottom of the vee. This primary orientation process was numerically modeled using a cylinder in point contact with 2 horizontal and parallel surfaces travelling at different velocities. The resulting analysis was used to study and select an optimum combination of product feed velocity, sizing belt velocity, and orienting belt velocities and velocity ratio.

A working prototype, which is now commercially available, was exhaustively tested in the laboratory and in long-term commercial operation. Utilization of the machine has been successfully extended to cucumbers and green peppers. Laboratory tests indicate that product sizing accuracy as high as 98% by number placed correctly can be expected over a wide range of feed rates.

A secondary orienting mechanism termed wobble was analyzed and developed. It incorporated 2 eccentrically bored sheaves placed π rad out of phase on a shaft to drive each pair of sizing belts. This drive was possible because of the ability of the polyurethane belts to stretch and contract. The eccentric drive produced an average sizing belt velocity with a cyclic velocity component superimposed. Tests indicated that the addition of wobble reduced sizing error significantly below that experienced with conventional drives. Other tests proved that varying the drive shaft speed to attain average sizing belt velocities in the range of 150 to 210 ft per min had minimal effect on sizing accuracy. These tests verified the results of the analytical study of primary product orientation. The analytical study also suggested an overall velocity ratio of 2.25 to 1 between the orienting belts. This ratio was used in all lab tests. It produced an orienting belt velocity combination which aided in product singulation and caused primary product orientation to be completed quickly and consistently. Product damage from the orientation-sizing process was negligible.

Laboratory tests proved that the machine could produce 2 or 3 size grades in a 6 ft length with acceptable accuracy. Product feed rates of 40 to 115 bu per hr per vee were also examined. Error was found to approximately triple as feed rate was doubled, but even at higher feed rates the error in no case exceeded 10.7%.   Order No. 75-5345, 81 pages.

CONICAL ELECTROSTATIC PROBE RESPONSE IN A WEAKLY IONIZED GAS FLOW

BRUCE, Charles Flick, Ph.D.
University of California, Berkeley, 1974

Conical electrostatic probes of lengths 0.153, 0.393 and 1.0 cm were placed in partially ionized argon flows in the laboratory in order to study the utilization of their current-voltage characteristics in the measurement of ion number densities over a wide range (from $n^i = 5.8 \times 10^7$ cm^{-3} to $n^i = 7.6 \times 10^{12}$ cm^{-3}). The ion densities and electron temperatures of the flows were measured with thin cylindrical electrostatic probes, and the neutral properties were determined from impact pressure, stagnation pressure and stagnation temperature measurements. The current-voltage characteristics of the ion-attracting conical probes were measured and compared to thin and thick sheath theories. Over the whole range of ion densities the measurements agreed reasonably well with the thin sheath theories of Chung and Blankenship (1966) and Denison (1967) which yield explicit expressions for the ion densities in terms

WAVEGUIDE EVANESCENT STREAK EXCITATION OF ADSORBED PROTEIN FLUORESCENCE

W. M. Reichert, K. Newby and J. D. Andrade

Department of Bioengineering, University of Utah, Salt Lake City, Ut 84112

A great deal of scientific effort is currently focused on the thrombogenic response to a material when it comes in contact with blood. Present theory suggests the most important event in blood/materials interactions is the initial deposition of blood plasma proteins. One of the established techniques for characterizing proteins adsorbed at the solid/liquid interface is Total Internal Reflection Fluorescence (TIRF). In this presentation we will discuss two new techniques similar to TIRF for evanescently exciting the fluorescence of proteins adsorbed to optical waveguide surfaces. The waveguides used are: 1) 1-3 μm polymer films spun cast onto pyrex substrates and 2) cylindrical glass multimode optical fibers. Both of these systems utilize an integrated optics modification of the evanescent excitation principle of conventional TIRF. Waveguide Evanescent Streak Excitation also measures the time dependent increase in protein fluorescence as the protein enters the evanescent volume and adsorbs at the solid/liquid interface. Rhodamine and Fluorescein labeled IgG served as the protein model.

Like TIRF, the evanescent field extending approximately 100-200 nm from the waveguide surface is produced by the total internal reflection of light. Unlike TIRF, a waveguide evanescent field will exist only for the discrete angles of total reflection that allow light to propagate down the waveguide. In integrated optical systems, light propagates down the waveguide interior by virtue of repeated total internal reflections. The summation of the repeated total internal reflections back and forth within the waveguide produces interference patterns or modes where each interference pattern is associated with specific angles of total reflection. Consequently, only those angles of total reflection that produce constructive interference patterns will allow light to propagate and only then will an evanescent field exist at the waveguide surface. The slab waveguide supports a limited number of propagating modes (1-5 modes for 1-3 μm polymer films) while a multimode optical fiber (600 μm diameter) supports greater than 10^4 propagating modes.

Slab waveguides spun cast from poly(styrene) and poly(methylmethacrylate) (Figure 1) offer some distinct advantages over conventional TIRF. Waveguide Evanescent Streak Excitation (WESE) provides: 1) a highly defined streak of evanescent excitation at the polymer surface, 2) a stronger interfacial evanescent intensity (at discrete coupling angles) than that obtained with the same laser intensity at the TIRF prism surface and 3) an exponential decay of the evanescent field which starts at the polymer waveguide surface and not below as in TIRF. These features produce improved signal/noise ratios, thus allowing one to use lower laser power and perhaps reduce the photobleaching problem. A flow system is currently being constructed to perform dynamic WESE fluorescence

of proteins adsorbed from a flowing solution to the polymer waveguide surface.

Cylindrical glass waveguides can be used as a remote evanescent sensor for protein adsorption. Here the sensor tip is formed by stripping the cladding from one end of a multimode optical fiber and capping the terminal end with an opaque epoxy to prevent light leakage out the end of the fiber core (Figure 2). When light is coupled in at the opposite end of the fiber it propagates to the sensor tip by total internal reflection, thus exposing the evanescent field at the surface of the stripped fiber core to the surround medium. When immersed in a protein solution the sensor tip evanescently excites and collects the fluorescence of proteins adsorbed to the sensor tip surface. The collected fluorescence then propagates back up the fiber for spectral analysis. This evanescent remote sensor shows feasibility as a "dip stick" immunosensor.

Experimental design and results will be presented. This work has been supported by a grant from The Office of Naval Research and NIH grants HL18519 and HL32132.
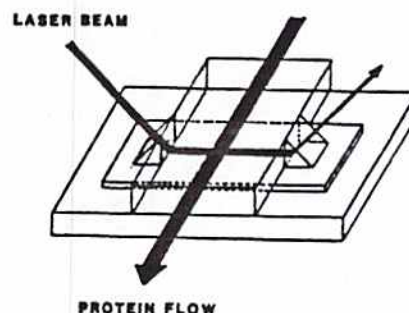

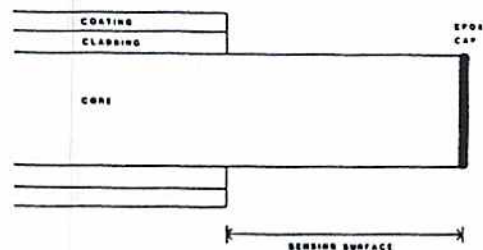Figure 1. Waveguide flow cell design for studying adsorbed proteins.

Figure 2. Sensor tip design showing the sensing surface and opaque terminating cap.

PROBING PROTEIN ADSORPTION: INTERFACIAL FLUORESCENCE AND GAMMA PHOTON DETECTION

Ab - Rein 1 '84
Interf. Fluorescen

D.R. Reinecke, R.A. Van Wagenen, J.D. Andrade, and L.M. Smith

Department of Bioengineering, University of Utah, Salt Lake City, Utah 84112

Total internal reflection interfacial fluorescence (TIRF) measurements are valuable for in situ probing of the quantity, activity, and conformation of protein adsorption at solid-liquid interfaces. Previous attempts to accurately determine with TIRF the quantity of adsorbed protein have relied on several assumptions; most significant is the insensitivity of fluorescence quantum yield to the adsorption process. We have developed a gamma photon counting system to measure protein adsorption in parallel with the TIRF system.

In TIRF, the excitation of the sample is accomplished by the evanescent wave of the internally reflected beam of the monochromatic, polarized light source. The intensity of the evanescent wave falls rapidly with distance t, $I_t = I_0 e^{-2t/\alpha}$ where I_0 is the intensity of the evanescing surface and α is a constant, with the resulting assumption that only a finite layer of sample ("interfacial") is contributing the majority of signal.

Following the development of Van Wagenen, et al. [1], the fluorescence quantum yield of the adsorbed protein, Q_A, can be related to that of the bulk solution, Q_B, as follows:

$$\frac{Q_A}{Q_B} = \frac{[FIU^2]T}{[FIU^2]I} \cdot \frac{N_A}{N_B} \cdot \frac{^{125}N_B}{^{125}N_A} .$$

Fluorescence counts for bulk and surface adsorbed protein are N_B and N_A, respectively; similarly, $^{125}N_A$ and $^{125}N_B$ are the counted γ-emissions of the ^{125}I radiolabelled protein. Evanescent wave intensity integrated across the sample volume is represented by $[FIU^2]T$ while $[FIU^2]I$ is that integrated over the adsorbed layer thickness. Clearly, after appropriate sampling geometry and efficiency corrections are applied to the detected gamma emission, the change in quantum yield upon adsorption can be determined.

The protein under study was human γ-globulin (Miles Laboratory) and low activity ^{125}I labelling was achieved by the relatively mild and easy lactoperoxidase-mediated procedure. Tryptophan residues of γ-globulin fluoresce at a wavelength of 335 nm when excited by UV light at 285 nm; this is termed intrinsic fluorescence as no labelling with a fluor is required.

The intrinsic TIRF instrumentation is configured identically to that described by Rockhold, et al. [2]. The flow cell was constructed of an elliptical Silastic ^{R} gasket (.75 mm thick) sandwiched between two hydrophilic quartz slides; cell volume was 0.8 ml and surface area was 22.0 cm^2. The prism-emission monochromator-photomultiplier tube (Hammamatsu) assembly was placed upon the prism side of the flow field, and the Bicron NaI(Tl) scintillator tube was placed on the other side of the flow cell. A template of 1.3 cm thick aluminum limited the Bicron sensing window to approximately

2.9 cm^2. Outputs of both detection systems were multiplexed to an Ortec photon counting system, and the data were transferred to an Apple II computer for manipulation and storage.

Experiments were performed with non-adsorptive Na ^{125}I to establish the overall efficiency at about 15%. Minimum detectability (defined as signal/$\sqrt{background} \geq 4$) was found to be activity of .008 µCi/ml. This sensitivity indicated that for an approximate surface adsorption concentration of .01 µg/cm^2 an initial labelling specific activity of 100 µCi/mg was required. Concentration effects were negligible as the efficiency remained nearly constant from samples of 5 µCi/ml to .008 µCi/ml. There was some concern that the radioisotope labelling procedure might quench the fluorescence of the γ-globulin, but studies with the protein cold-labelled with nonradioactive I^- showed no significant change in the fluorescence spectrum. Additionally, the bound I^- was very stable with little dissociation for periods up to one week.

An essential criterion for these experiments is that radiolabelling does not alter the adsorption properties of the γ-globulin. A previous study has shown that labelling of this protein should indeed not affect its adsorption [3]. Experiments now in progress will verify this for our system; varying the fraction of labelled and unlabelled bulk γ-globulin is predicted to equivalently alter the quantity of detected gamma emission.

If the quantum yield remains constant, the relationship between gamma emission and fluorescence counts for both bulk and adsorbed protein is predicted to be the constant ratio of the field intensities. Preliminary experiments with γ-globulin labelled to an undetermined specific activity show a good linearity with protein concentrations < .1 mg/ml. This suggests that even if there is a change in quantum yield it should be constant and, therefore, easily determined by using γ-globulin of well-characterized specific activity. These investigations are now underway. Some light should also be shed on possible mechanisms of quenching such as adsorbed concentration, temperature, pH, and type of buffer.

1. Van Wagenen, R.A., et al., Biomaterials, Cooper, S.L. and Peppas, N.A., Eds., ACS Adv. Chem. Series, 1981.
2. Rockhold, S.A., et al., J. Electroanal. Chem., 150, (1983) 261.
3. Crandall, R.E., et al., Prep. Biochem., 11, (1981) 113.

ADSORPTION OF HUMAN LIPOPROTEINS TO SILICA SURFACES

J. Rickel, V. Hlady, and J.D. Andrade

Department of Bioengineering, University of Utah, Salt Lake City, Utah
84112

Plasma lipoproteins are lipid-protein complexes responsible for the transport of water insoluble lipids in the circulation. They can be pictured as an apolar ion, composed mainly of triglycerides and cholestrol esters, surrounded by amphiphilic components, unesterified cholesterol and proteins known as apolipoproteins, providing a barrier between the aqueous medium and the hydrophobic region (1). The importance of lipoproteins in the initial exposure of a foreign surface to blood was indicated recently by a study showing that high density lipoprotein (HDL) preferentially adsorbs from plasma onto polyvinyl chloride and polystyrene surfaces (2). Such preferential adsorption of HDL causes lower adsorption of albumin, fibrinogen, and immunoglobulin from plasma compared with their adsorption from pure protein solutions. Other investigators have observed that iodinated low-density lipoprotein (LDL) binds strongly to glass beads at physiologic pH and ionic strenth, but that treatment of the beads with silicone virtually eliminates the high affinity binding (3). In the presence of thrombin, LDL enhances platelet aggregation, whereas HDL decreases aggregation (4). These characteristics, as well as the part these two main classes of lipoproteins play in atherosclerosis (LDL is the major vehicle for the transport of cholesterol in man), prompted this study of their adsorption behavior, using the intrinsic fluorescence of their apolipoproteins as the measured parameter.

Lipoprotein density classes were isolated by sequential ultracentrifugation from freshly-drawn, whole human serum. Density of the serum was adjusted by the addition of solid KBr. LDL was isolated between $\delta = 1.030 - 1.063$ g/cm^3 and HDL, between $\delta = 1.063 - 1.230$ g/cm^3. Lipoprotein adsorption was followed via the intrinsic fluorescence of tryptophans in their apolipoproteins, using the total internal reflection intrinsic fluorescence (TIRIF) method. This method utilizes the evanescent surface wave created by total internal reflection of UV light (285 mn) at the quartz/electrolyte interface (5). The photoenergy available for the excitation of tryptophans in the sample decays exponentially into the solution, thus allowing monitoring of lipoprotein fluorescence from the adsorbed layer. The adsorption of HDL and LDL was studied from PBS and from Dulbecco PBS buffer (containing divalent cations) onto hydrophilic silica or onto silica made hydrophobic by solution coating with dimethyldichlorosilane (DDS).

We found that the adsorbed amount of LDL exceeded that of HDL on both types of surfaces and in both buffers on hydrophilic silica. However, HDL is composed of 50% protein and 50% lipid constituents while LDL is only 20% protein and 80% lipid. In assaying the amount of protein adsorbed, the amount of HDL protein adsorbed exceeded that of LDL protein. Further studies are needed to determine which of the lipoprotein components is responsible for adsorption of the particle.

We also found that the adsorbed amounts of both HDL and LDL were lower on hydrophobic silica. This may indicate differences in the binding mechanisms to hydrophilic and hydrophobic surfaces. Under certain experimental conditions, a higher percentage of adsorbed protein was removed from the surface during desorption. In the case of HDL, the amount remaining bound to either a hydrophobic or hydrophilic surface after a 30-minute PBS flush decreased with increasing concentration of the original adsorption solution. This indicates that bombarding a surface with lipoprotein particles more quickly may decrease the chances for protein reorientation, thus allowing increased desorption due to weaker binding. LDL showed a similar, less marked trend only on hydrophilic silica. For both lipoproteins adsorbed onto hydrophilic silica from PBS, the concentration remaining after a 30-minute buffer flush was proportional to the maximum adsorbed amount detected. This was also true for LDL in PBS on DDS.

We conclude that the adsorption behavior of lipoproteins onto hydrophilic and hydrophobic surfaces is probably due to the fact that it is the protein moieties which are interacting with the material surface. On hydrophilic surfaces, adsorption is probably due to electrostatic charge interactions with hydrophilic amino acids on the apolipoprotein. Hydrophobic interactions with the hydrophobic faces of apolipoprotein α-helices probably cause the binding of lipoproteins to hydrophobic surfaces. This may involve some reorientation of the helices. HDL apolipoproteins are known to contain amphipathic helices whose normal orientation in the lipoprotein puts their hydrophilic face toward the aqueous surroundings (1). Binding of HDL particles to either surface may require the reorientation of these helices. A hydrophobic surface would require a greater amount of protein conformational change and would thus be a less favorable surface for adsorption. Little is known about the sequence or structure of the LDL apolipoprotein, but its binding is probably defined by these same parameters.

References:

1. Mantulin, W.W. and H.J. Pownall, in Excited States of Biopolymers, R.F. Steiner, ed., Plenum Press, New York, 1983, 163-202.
2. Breemhaar, W., E. Brinkman, D.J. Ellens, T. Beugeling, and A. Bantjes, Biomaterials 5 (1984) 269-274.
3. Dana, S.D., M.S. Brown, and J.L. Goldstein, Biochem. Biophys. Res. Commun. 74 (1977) 1369-1376.
4. Auiram, M. and J.G. Brook, Atherosclerosis 4b (1983) 259-268.
5. Hlady, V., R.A. VanWagenen, J.D. Andrade, Protein Adsorption, J.D. Andrade, ed., Plenum New York, 1985, 81-120.

Abstract Submitted

for the <u>March</u> Meeting of the

Americal Physical Society

<u>March 21-24, 1977</u>
Date

Physics and Astronomy
Classification Scheme
Number <u>81</u>

Bulletin Subject Heading
in which Paper should be
Placed:
<u>High Polymer Physics</u>

<u>Effect of Hydrogen-Bonding on Sub-T_g Relaxations
in Hydrophilic Methacrylate Polymers.</u> G.A. RUSSELL[+], P.A.
HILTNER[+], and J.D. ANDRADE[+], [+]University of Utah, [+]Case
Western Reserve University.*--Dielectric Relaxation
studies were carried out from 77°K to 300°K and from 10
Hz to 10 KHz on poly(2-hydroxyethyl methacrylate) [HEMA]
polymers and poly(2-methoxyethyl methacrylate) [MEMA]
polymers of varying degrees of stereoregularity. The
effect of the hydrogen-bondable hydroxyl side-chain of
HEMA was twofold. First, T_γ, the temperature of the
lowest temperature dispersion, was raised by 20-30°K for
HEMA when compared to MEMA, which cannot hydrogen-bond.
Second, the energy of activation of the γ relaxation was
~1 kcal/mole higher for HEMA than for MEMA, indicating
that hydrogen bonds increase the effective size of the
kinetic unit which gives rise to the dispersion. Activa-
tion energies and T_γ for HEMA and MEMA are comparable to
those obtained by dynamic mechanical techniques.[1]
*Supported by NIH Grant No. HL16921.
[1]M.C. Shen, J.D. Strong, and F.J. Matusik, <u>J. Macromol.
Sci.</u> (Phys.), B1, 15 (1967).

Submitted by

Note: Either a poster session
or regular session will be
acceptable to me.

Geoffrey A Russell
Signature of APS Member

Geoffrey A. Russell
Same Name Typewritten

Department of Materials Science & Eng.
Address
University of Utah
Salt Lake City, Utah 84112